AN INTEGRATED ZONAL MODEL TO PREDICT TRANSIENT INDOOR HUMIDITY DISTRIBUTION

Hui Zhao

A Thesis

in

The Department

of

Building, Civil and Environmental Engineering

Presented in Partial Fulfillment of the Requirements
for the Degree of Master of Applied Science at
Concordia University
Montreal, Quebec, Canada

July 2004

Your file Votre référence
ISBN: 0-612-94683-5
Our file Notre référence
ISBN: 0-612-94683-5

ABSTRACT

An Integrated Zonal Model to Predict Transient Indoor Humidity Distribution

Hui Zhao

Indoor air humidity has been recognized as an important environmental parameter, which can greatly affect the quality of indoor environment, durability of building construction component and interior furnishings, building energy consumption and the state of occupants as well as their health. Until recently, most of existing indoor humidity evaluation models were strictly based on the mass balance between humidity generation rate and humidity dilution by air leakage, ignoring moisture absorption and desorption by interior surface. This could lead to considerable inaccuracy in the predicted humidity level.

To investigate the impact of building material moisture adsorption and desorption on indoor air humidity and predict humidity distribution in a room, a zonal model was integrated with building material moisture transfer model. This integrated zonal model was developed based on the conservation of air mass, energy and water vapor mass. The model was applied to a room with forced or natural convection airflow. The model could predict humidity and temperature distribution in the room and showed the influence of building material moisture adsorption and desorption on this behavior. It was found that moisture adsorption and desorption by building materials not only influenced humidity

distribution within the room but also affected the moisture content in the building materials.

The predictions of the integrated zonal model were compared with the available data in the literature. The comparisons indicated that there were generally good agreements between the proposed model predictions and literature results. The results also showed that the integrated zonal model, with quite coarse mesh, could provide sufficiently reliable information about airflow pattern, thermal and indoor humidity distributions within a room.

Finally, the model could be used to analyze building material moisture adsorption and desorption behaviors and provide useful information for building owners or designers on selecting proper building materials, designing efficient ventilation systems and assessing indoor air quality.

Keywords: zonal model, moisture transfer model, indoor humidity, building materials, moisture adsorption/desorption

ACKNOWLEDGMENTS

I wish to express my sincere thanks and appreciation to my supervisor Dr. F. Haghighat for his encouragement and help.

Special thanks go to Dr. Hongyu Huang for her endless advice and fruitful discussions regarding to the whole research work.

Extended thanks go to all my friends and colleagues at Concordia University for their sincere help and good companies throughout these years.

Last, but not least, to my whole family, especially to my parents, and my husband, Xueyan Guo, my son, Tianyu, my daughter, Chenxi for their unconditional love, supports, understanding and encouragements.

TABLE OF CONTENTS

LIST OF FIGURES

Chapter 2

Chapter 3

LIST OF TABLES

LIST OF SYMBOLS

English letters

A area of interface, m^2

A_e exposed area, m^2

C gas-phase concentration, kg/m^3_{gas}

C_{ad} adsorbed-phase concentration, $kg/m^3_{material}$

$C_{ad,s}$ the mono-layer surface saturation concentration.

C_d coefficient of Power law, usually taken as 0.83, $kg/s \cdot P_a^n$

C_p air specific heat, $J/kg \cdot k$

C_m material moisture capacity, $kg/kg \cdot Pa$

c_o water vapor content in the air supply, kg/m^3

c_i water vapor content in the room air, kg/m^3

D material moisture diffusivity, m^2/s

D_{ad} adsorbed- phase or surface diffusion coefficient, m^2/s

D_g gas phase diffusion coefficient due to molecular and /or Knudsen diffusion,

m^2/s

D_p overall moisture diffusion coefficient, m^2/s

D_v vapor permeability, $kg/m \cdot Pa \cdot s$

d	effective penetration depth, m
G	moisture generation rate, kg/s
g	gravitational acceleration, m^2/s
H	height of the cell i, m
h_c	convective heat transfer coefficient, $w/m^2 \cdot k$
h_m	convection mass transfer coefficient, m/s
K	dimensionless adsorption equilibrium constant
K_{BET}	BET equilibrium adsorption constant
K_F	Freundlich's equilibrium adsorption constant
K_H	Henry adsorption equilibrium constant
K_L	Langmuir's equilibrium adsorption constant
k	thermal conductivity, $w/m \cdot k$
l	cell's dimension perpendicular to the interface, m
M_i	mass in cell i, kg
M	rate of moisture absorbed on the room surfaces, kg/s
m_{ij}	mass flow across cell i and cell j interface, kg/s
$m_{ij,hor}$	airflow rate across horizontal boundary, kg/s
m_{0-Z_n}	airflow rate under neutral plane, kg/s
m_{source}	rate of mass generated in cell i, kg/s
$m_{\sin k}$	rate of mass removed from cell i, kg/s
m_{wv}	water vapor mass flow rate, kg/s

m_{wv} moisture adsorption/desorption rate, kg/s

$m_{wv,source}$ water vapor source, kg/s

$m_{wv,\sin k}$ water vapor sink, kg/s

m_{Z_n-H} airflow rate above neutral plane, kg/s

m_{ver} total airflow rate across vertical boundary, kg/s

N air changes, s^{-1}

n flow exponent, usually taken as 0.5

P total pressure, Pa

$P_{i,h}$ pressure at the height of h in cell i, Pa

P_m partial vapor pressure within materials, Pa

$P_{ma,i}$ total pressure of the cell i, Pa

$P_{middle,i}$ pressure at the middle of cell i, Pa

P_V partial vapor pressure, Pa

$P_{ref,i}$ reference pressure of cell i, Pa

ΔP_{ij} pressure difference between cell i and j, Pa

ΔP_{ref} difference of the reference pressure between the cell i and i+1, Pa

Q_i heat in cell i, J

q rate of moisture flow, $kg/m^2 \cdot s$

q_{ij} heat flow across cell i and cell j interface, W

q_{source} rate of energy generated in cell i, W

$q_{\sin k}$ rate of energy removed from cell i, W

R gas constant of air, $287.055\ J/kg \cdot k$

T temperature, K

T_i temperature of cell i, K

T_j temperature of cell j, K

ΔT_{i-wall} temperature difference between cell i and wall, K

t time, s

V the volume of the room, m^3

V_m material volume, m^3

v volume of the cell, m^3

x, y, z distance in different directions, m

Z_n the height of the neutral plane, m

Greek letters

α_F the order of adsorption

ρ material density, kg/m^3

$\Delta\rho$ difference of the density between the cell i and i+1, kg/m^3

ρ_i density of the cell i, kg/m^3

ρ_{in} water vapor density in the inlet air, kg/m^3

ρ_m water vapor density in the materials, kg/m^3

ρ_{m0} initial water vapor density in the material, kg/m^3

ρ_{wv} water vapor density in the cell air, kg/m^3

ρ_{wv0} initial water vapor density in the room air, kg/m^3

ω angular frequency, s^{-1}

δ_v water vapor permeability in the material, m^2/s

γ viscosity, $kg/m \cdot s$

i refer to face i of the cell

Chapter 1

INTRODUCTION

1.1 Background

Nowadays, as people spend most of their time in enclosed spaces, concerns and interests have increased dramatically in the problems dealing with indoor air quality. Meanwhile, some studies have shown that one of the most influential parameter is moisture content in the indoor air. Indoor air humidity, as an important environmental parameter, can affect building performance in many aspects including the quality of the indoor environment, the durability of building construction component and interior furnishings, building energy consumption, and comfort of occupants and their health.

The ASHRAE Standard 62 (ASHRAE, 2001) recommends an optimum indoor humidity range of 30% - 60%. ASHRAE Standard 55 (ASHRAE, 1992) prescribes a low humidity ratio limit of 4.5g/kg, which is also about 30% relative humidity at 20°C. The low relative humidity limit presented in the two standards is set in order to minimize dry eyes, noses irritation, difficulty in breathing, allergy, asthma and other related problems. In addition, low indoor relative humidity also could result in the cracking and flaking of moisture sensitive materials. On the contrary, an excessive humidity can increase indoor contamination levels, which can cause rotting and unpleasant odors, and reduce indoor air quality. It has been found that airborne bacteria and some other indoor contaminants such

as formaldehyde will be more active at relatively higher indoor humidity levels (Kelly, 1982). Furthermore, in cold climates internal surface condensation is a likely consequence of high humidity. It can cause mildew growth as well as damage decorative finishes and building structures.

In many situations, indoor air humidity is required to be maintained at a certain constant level. In order to achieve this goal, indoor air has to be continuously humidified or dehumidified by air-conditioning systems at the price of energy consumption. Also in recent years, the desire for reduced energy consumption in buildings has resulted in a great degree of separation between the indoor and outdoor environment by reducing air leakage through the building envelope and increasing its thermal resistance. Therefore, it introduced many new problems related to durability and maintenance as well as the quality of the indoor air.

Generally, indoor air humidity is determined by the balance between moisture gains and losses within the enclosed indoor air space. Depending on the building type and its functional characteristics, moisture can be gained and lost from the space by occupants and their activities, surface evaporation and condensation from damp materials or free water surfaces, mechanical ventilation system, and moisture adsorption/ desorption by interior hygroscopic materials. The most commonly used method of predicting indoor air humidity is based on mass balance between the rates of moisture generation and loss due to ventilation and air leakage at steady state (Kusuada, 1983). Moisture adsorption and desorption by the interior surface and furnishings was not taken into account. However,

water vapor generated in the room can be absorbed by furniture and construction materials. This means that the cooling load used to control humidity peak levels can be considerably overestimated without considering moisture adsorption and desorption by interior surface. This can lead to considerable inaccuracy in the predicted humidity level since as much as one third of the moisture generated in a room could be absorbed by its surfaces (Kusuada, 1983). Therefore, it can result in inaccuracies in building energy analysis and poor indoor air quality.

For better assessment of the indoor air quality and more accurate prediction of energy consumption in buildings, the dynamic nature of indoor air humidity must be considered.

Generally, the existing methods to predict indoor air humidity distribution are the experimental method and the numerical method. Due to the conditional limitations of the experimental method, the numerical method is more practical and powerful. The Computational Fluid Dynamics (CFD) method is well-known and is used extensively. It can accurately simulate airflow pattern, temperature, and contaminant distribution within a room; however, it is too complicated and time consuming. Another commonly used numerical method is the zonal model. Compared to CFD models, the zonal model is easier to use, time saving, and computationally efficient.

In summary, this study will focus on integrating the zonal model to consider the effect of the moisture adsorption and desorption of interior materials on indoor air humidity distribution within a room.

1.2 Objectives of Research

The main objectives of the present research can be summarized as following:

1. Carry out a critical review of moisture transfer mechanisms and the existing theoretical models within porous materials, interaction between indoor air and furnishing materials, and indoor air in order to find the most appropriate modeling approach to describe the moisture transfer process.
2. Integrate Zonal Model to predict transient behavior of indoor air humidity and its distribution within a room by taking into account the effect of adsorption and desorption phenomena.
3. Use the proposed model to study the effect of building material moisture adsorption/ desorption on indoor air humidity distribution and on building material moisture distribution.

Therefore, the present research will provide designers and manufacturers with a better understanding of the effect of building materials moisture adsorption and desorption on the indoor air humidity; ultimately, it can contribute to the reduction and prevention of the Indoor Air Quality related problems and energy consumptions.

1.3 Methodology of Research

To achieve those objectives, the following tasks must be carried out:

1. Develop a moisture transfer model to predict moisture transfer in building materials.
2. Integrate this moisture transfer model with a Zonal Model to predict the dynamic behavior of indoor air humidity distribution in a room, taking into account the effect of the adsorption/ desorption phenomena.
3. Carry out case studies to investigate the effect of interior surface moisture transfer on indoor air humidity distribution.

Chapter 2

LITERATURE REVIEW

2.1 Introduction

The role of indoor air humidity as an environmental parameter affecting the energy consumption and the quality of indoor environment as well as the occupants' thermal comfort and their health has been discussed in the previous chapter. However, indoor air humidity is a function of many interrelated moisture transport processes that depends on building physical and functional characteristics. A comprehensive literature review suggests that building materials can affect the transport and removal of indoor moisture through the adsorption and desorption process. For better understanding and appreciation of indoor humidity distribution and its impacts on people's health and building energy consumption, the actual moisture transport process and mechanism from building materials to indoor air must be known.

This chapter reviews both experimental methods and theoretical models used to study moisture transport and mechanism through the building materials, moisture adsorption and desorption, and moisture transport and distribution in the indoor air. At the end of the chapter, the main achievements as well as the limitations of existing methodologies are highlighted and analyzed. As a result, it will lead to the development of a suitable model for evaluating the indoor humidity behaviors and distributions in the room.

2.2 Literature Related to Moisture Transfer in Envelope System

Most building materials are porous medium (Kumaran, 1992). All porous media are occupied by solid matrix and void space that is filled by fluid phase (Bear and Bachmat, 1990). Because of these void spaces, porous material can be expected to retain water vapor for a considerable amount of time. The absorbed water will later be released when the outside weather is warmer, or it will be released by diffusion into the relatively dry air outside. Normally, moisture can exist in the building porous materials in one or more of its forms (i.e. water vapor, liquid, and solid). Knowledge of moisture transport mechanisms through building porous materials is the first step towards understanding its impact and interaction with indoor air.

2.2.1 Moisture transport mechanism and driving potentials

2.2.1.1 Driving potentials

In his state of the art review, Straube and Burnette (2001) points out that there is a range of variables used as moisture driving potential. These include partial vapor pressure, capillary suction pressure, moisture content, and temperature.

The disadvantage of using the moisture content as the driving force is that it is discontinuous at material interfaces. Hence, it requires recalculating the moisture content into another driving potential at the boundaries between different layers. The capillary suction is likewise a continuous function, but it is not easy to measure, especially when

the relative humidity exceeds 98%. As a driving potential, temperature is easy to measure; however, temperature gradient is the only potential used for heat transfer since it will induce thermally driven vapor diffusion.

2.2.1.2 Moisture transport mechanism

Moisture can migrate in porous materials in either vapor (gas-phase) or liquid (liquid-phase) forms. Therefore, water vapor diffusion, being the most common mechanism of moisture transfer in porous building materials, has received particular attention in literatures (ASHRAE Fundamentals, 2001; Diasty *et al.*, 1993; Swami and Chandra, 1988). Vapor (gas-phase) diffusion includes molecular diffusion and Knudsen diffusion (effusion). The relevant driving force for vapor diffusion is the vapor pressure gradient (Spooner, 1983). In a more comprehensive study (Andesson, 1985), both experimental and theoretical approaches were utilized to investigate moisture transport (mainly vapor diffusion) in different building materials. On the other hand, Straube and Burnette (2001) found that Knudsen diffusion was explicitly ignored by most heat and moisture transfer models used in building technology.

Conversely, in some building components, especially those exposed directly to the outdoor environment, liquid transport becomes significant, which includes by surface (adsorbed-phase) diffusion and capillary flow. Surface diffusion, as an important transport mechanism, has been addressed in a series of studies (Hall, 1977, 1984, 1986, l'Anson and Hoff, 1986). Surface diffusion takes place in the absorbed water layer of the

material surface. Ojanen *et al.* (1989) described the phases of moisture sorption in pores of materials as the concentration increases, as shown in Figure 2-1. At low concentration, moisture exists as water vapor (gas-phase) and adsorbed-phase, but transfer takes place by only vapor diffusion (Figure 2-1 (a)). As the concentration increases, the thickness of adsorbed layer increases and both water vapor (gas-phase) and adsorbed-phase diffusions occur (Figure 2-1(b)). Then capillary condensation takes place in small pores and the adsorbed layer gets thicker when vapor, adsorbed-phase diffusion, and capillary flow all coexist (Figure2-1 (c) and (d)). As pores are filled with condensed water, vapor and adsorbed-phase diffusion no longer take place (Figure 2-1 (e) and (f)).

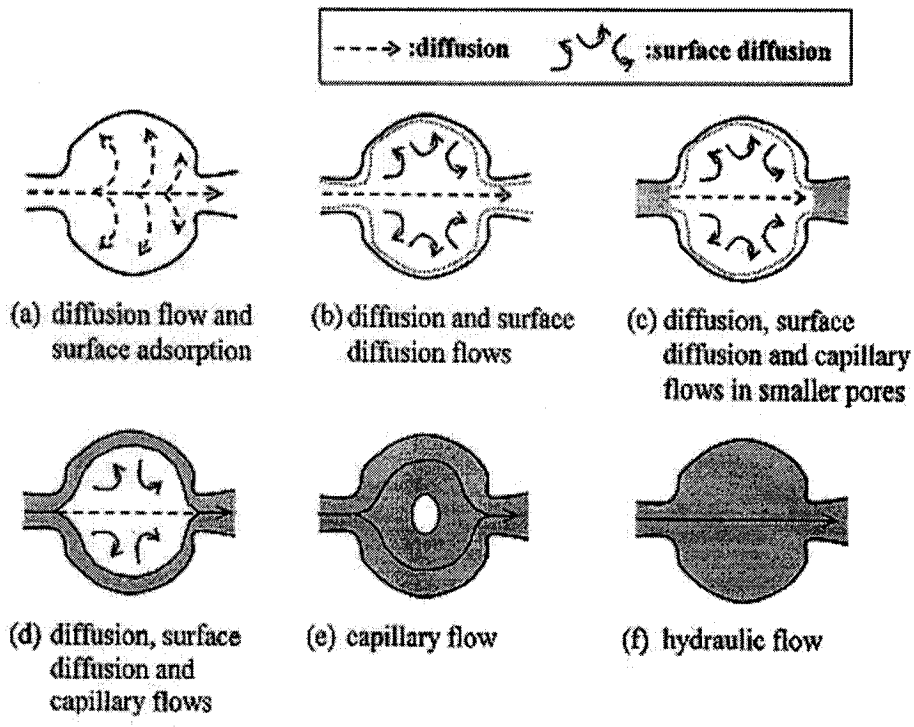

Figure 2-1 Phase of moisture sorption (from Ojanen et al., 1989)

In summary, moisture flow in porous materials cannot simply be driven by vapor diffusion or capillary suction; meanwhile, surface diffusion also acts and all three mechanisms may be acting at the same time (Straube and Burnette, 2001).

Therefore, in this study, moisture transfer in porous materials will focus on gas or vapor diffusion and surface diffusion. Vapor diffusion means molecular diffusion and surface diffusion are adsorbed-phase diffusions.

2.2.1.3 Diffusion coefficients' estimation

Evaluation of vapor diffusion coefficients has been the subject of many studies (Andesson, 1985, Kumaran, 1989, Hansen and Bertelsen, 1989). A widely accepted method for evaluating materials' vapor diffusion coefficient is the cup method that is adopted by ASHRAE Fundamentals (2001). Meanwhile, when there is significant adsorption on the pore wall, surface (adsorbed-phase) diffusion will become important. However, if adsorbed molecules are held so strongly as to be essentially immobile, surface diffusion will be insignificant (Satterfield, 1970).

The flux of the gas phase and adsorbed phase are parallel and additive so that the overall diffusion coefficient can be calculated by the sum of the vapor diffusion coefficient and surface diffusion coefficient by considering the adsorption. That can be expressed as follows (Ruthven, 1984),

$$D_p = D_g + K \cdot D_{ad} \qquad (2\text{-}1)$$

Where,

D_p : overall moisture diffusion coefficient, m^2 / s

D_g : gas phase diffusion coefficient due to molecular and /or Knudsen diffusion, m^2 / s

D_{ad} : adsorbed- phase or surface diffusion coefficient, m^2 / s

K : dimensionless adsorption equilibrium constant

The adsorbed-phase or surface diffusion coefficient, D_{ad}, varies between 10^{-7} and 10^{-17} m^2 / s depending on the types of adsorbate and adsorbent (Satterfield, 1970). The contribution of the surface diffusion to the overall diffusion coefficient depends on the ratio of the product of $K \cdot D_{ad}$ to D_g. In most macro porous building materials, molecular diffusion dominates and D_g is generally much larger than D_{ad} (Lee, 2003). In addition, macro pores typically contribute very little to adsorption capacity (Karger and Ruthven, 1992); hence, K will be relatively small. Therefore, surface diffusion will be negligible in macro porous building materials, unless there is significant adsorption.

2.2.2 Heat, air, and moisture transport model (HAM Model) review

Based on moisture transport mechanisms, many Heat, Air, and Moisture (HAM) transport models have been developed for predicting moisture transportation in building materials. They are briefly reviewed below.

2.2.2.1 Steady state model

In ASHRAE Fundamentals (2001), a steady state model is described, which uses Dew-point method or Glaser diagram to predict moisture condensation within building envelopes. Both methods are based on the following assumptions:

1) Boundary conditions are in steady state;

2) Water vapor diffusion is one dimensional and perpendicular to building envelope.

The Dew-point method does not contain a calculation of the moisture transfer; it simply checks and compares the temperature of sensible layers with the dew point of the environment of the construction. Glaser's method was originally a graphical method (Pedersen, 1992), which was developed in 1959 to determine the distribution of vapor pressure through a construction. It considered vapor diffusion according to Fick's law using constant material properties. Glaser diagram has been applied to all kinds of building envelope parts, irrespective of materials, the presence or absence of cavities, and built in moisture (Hens, 1996). The success of Glaser diagram is that a construction element can be quickly judged on its suitability: indoor vapor pressure, above which condensation starts, can be defined in a straight way in the form of diffusion resistance vs. water vapor pressure. However, the application of the diffusion approach is limited to certain building envelopes and thereby, the application of the steady state methods is severe (ASHRAE Fundamentals 2001).

2.2.2.2 Transient models

Cunningham (1990a) uses a simplified approach and develops a finite difference model. He consideres water vapor pressure to be the only driving potential. The moisture transport mechanism is given by Equation (2-2).

$$q = -D_V \frac{\partial P_V}{\partial x} \qquad (2\text{-}2)$$

Where,

q : rate of moisture flow, $kg / m^2 \cdot s$

x : distance, m

D_v : vapor permeability, $kg / m \cdot Pa \cdot s$

P_V : partial vapor pressure, Pa

The model couples moisture content with water vapor pressure and a linearly varying vapor diffusion coefficient through the sorption isotherm. Simulation results of this model are validated by laboratory tests under certain conditions (Cunningham, 1990b). The limitations of the model are that it cannot deal with rain adsorption, when capillary active materials are above the critical moisture content or there are complex airflows.

Compared with the models that only consider water vapor diffusion or liquid flow, MOIST model (Burch *et al.*, 1995a) takes into account both vapor diffusion and liquid flow. This one-dimensional hygrothermal model includes water vapor flow driven by vapor pressure gradients and capillary transport driven by capillary pressure gradients. Both water vapor permeability and hydraulic conductivity are assumed as functions of

moisture content. A good agreement is shown between the predictions made by MOIST and simple laboratory validation tests in the hygroscopic range (Burch *et al.*, 1995b). However, the precision of predicted results is determined by the number of nodes defined for each layer; that is, MOIST allows only a number of equally spaced nodes in each layer.

Another commonly used window-based model is called WUFI ORNL/IBP (Kuenzel and Kiessl, 1997), which is a one-dimensional transient hygrothermal model. In this model, water vapor diffusion and liquid water transport are both considered, and water vapor pressure and relative humidity are assumed to be driving potentials, respectively. One of the most important characteristics of this model is that it uses a full moisture retention function from the sorption isotherm and suction curve. This means it can cover the whole range of relative humidity from oven dry to 100% relative humidity. Another important feature of this model is its ability to incorporate driving rain deposition as part of its boundary conditions, the use of different liquid moisture diffusivities for wetting and drying/redistribution processes. The predictions of this model have good agreement with experimental data (Kuenzel and Kiessl, 1997). The major limitations are that it lacks ability to handle air leakage, associated energy, and moisture flow; meanwhile, relative humidity as driving potential also confuses users because of its vague physical meaning.

Another two-dimensional advanced hygrothermal model is hygIRC Model (Maref *et al.*, 2002), which is developed by the Institute for Research in Construction (IRC) at the National Research Council, Canada (NRCC). Compared to other models, this model

takes the influence of air on moisture transport into account and used the most complete moisture storage function. This model consideres vapor and liquid transport separately; where, water vapor diffusion is determined by the gradient of water vapor pressure and water vapor permeability. Liquid water transport is calculated by the gradient of moisture content and moisture diffusivity.

There are many other moisture transport models such as TCCCD2 (Ojanen *et al.,* 1989, 1994), FSEC (Keresteciogl u, 1989), MOISTURE-EXPERT (Karagiozis, 2001), UMIDUS (Mendes *et al.*, 1999, 2001), and Delphin (Grunewald and Houvenaghel, 2000) describes the heat and moisture transfer within building envelops and they have different capacities.

The main limitation of HAM (Heat, Air and Mass) models is to use prescribed indoor conditions (relative humidity and temperature), without considering the interaction between indoor air and building materials. In other words, existing models ignores the effect of indoor air humidity on wall moisture performance by assuming constant indoor humidity conditions and the lack of information about the influence of wall moisture performances on indoor air quality.

2.3 Adsorption and Desorption

2.3.1 Principle of adsorption and desorption

In general, most porous materials, in particular building materials, interact with ambient moisture through adsorption and desorption process (ASHRAE Fundamentals, 2001). Adsorption is a process where molecules from a gas phase or from a solution bind in a condensed layer on a solid or liquid surface (Masel, 1996). In other words, adsorption is the accumulation of gas, vapor or liquid (adsorbate) on a solid or liquid surface (adsorbent). One possible explanation of this phenomenon is that the adsorption process results from the interaction between a gas and a solid surface which continues until a thermodynamic equilibrium is achieved between the gas phase and adsorbed layer (Quenard and Sallee, 1991). If no more moisture transfer occurs between the material and its surroundings, the material is in equilibrium with the environment. When equilibrium is reached, the amount of moisture that is adsorbed depends on the temperature, pressure, and composition of the gas. The relation between partial vapor pressure (or more often relative humidity, RH) of the surroundings and the moisture content in the materials is called the sorption curve (Kumaran, Annex24). Sorption isotherms for a few construction materials are available in literature (Keresteciogl*u et al.*, 1998). As shown in Figure2-2, there are significant differences between different materials, and it depends on the average pore size and the pore-size distribution of the materials.

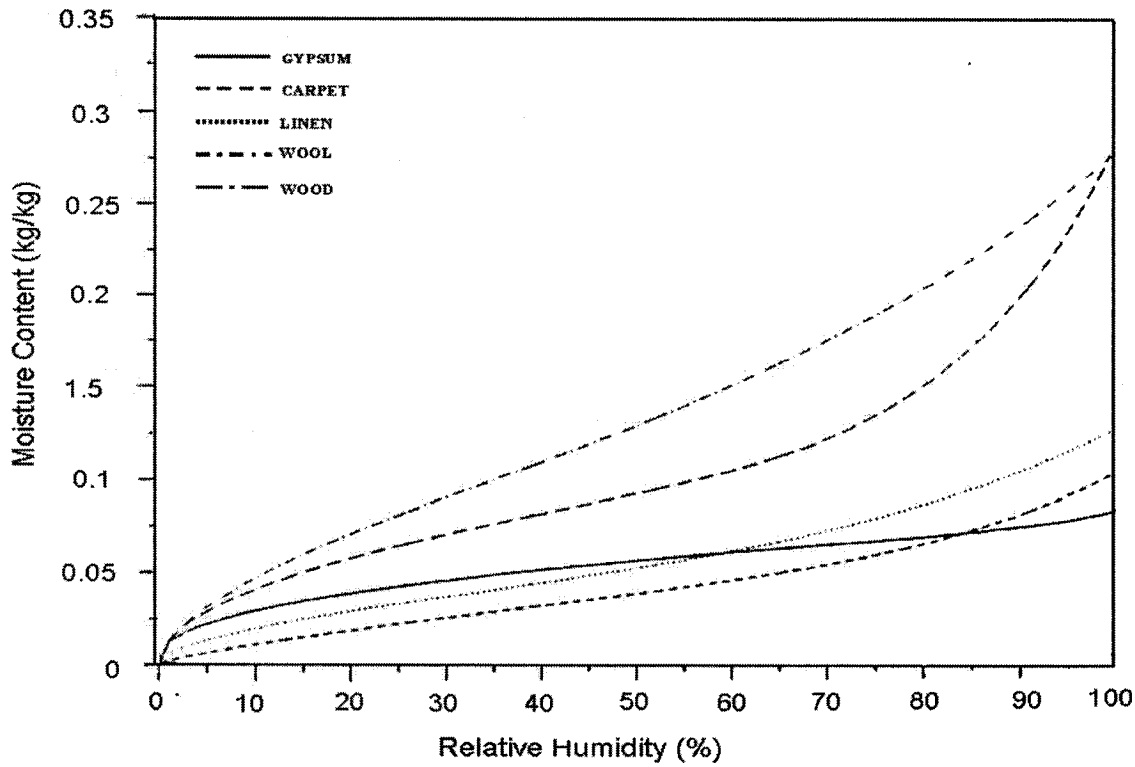

Figure 2-2 Sorption isotherms (wetting) for a few materials (from Keresteciogl u et al, 1998)

Adsorption isotherm also can be used to describe sorption in porous materials. It shows the dependence of adsorbed-phase concentration on the gas-phase concentration in the equilibrium state at a constant temperature (Lee, 2003).

$$C_{ad} = f(C,T) \qquad (2\text{-}3)$$

Where,

C_{ad} : adsorbed-phase concentration, $kg / m^3_{material}$

C : gas-phase concentration, kg / m^3_{gas}

T: temperature, K

The generally applied models for the sorption isotherms are reviewed as follows (Young and Crowell, 1962; Ruthven, 1984; Axley, 1991):

- Henry isotherm describes a linear relation. At low concentration level, all isotherms can be regarded as linear.

$$C_{ad} = K_H \cdot C \tag{2-4}$$

Where, K_H is Henry adsorption equilibrium constant.

- Freundlich isotherm is an empirical model that can be applied to nonlinear regions of high concentration level.

$$C_{ad} = K_F \cdot C^{\alpha_F} \tag{2-5}$$

Where, K_F is Freundlich's equilibrium adsorption constant; and α_F is the order of adsorption.

- Langmuir isotherm is the simplest theoretical model for monolayer adsorption.

$$C_{ad} = \frac{K_L \cdot C_{ad,s} \cdot C}{(1 + K_L \cdot C)} \tag{2-6}$$

Where, K_L is Langmuir's equilibrium adsorption constant; and $C_{ad,s}$ is the mono-layer surface saturation concentration.

- BET (Brunauer, Emmett, and Teller) isotherm accounts for the multi-layer adsorption.

$$C_{ad} = \frac{K_{BET} \cdot C_{ad,s} \cdot (\frac{C}{C_s})}{(1 - \frac{C}{C_s}) \cdot (1 - \frac{C}{C_s} + K_{BET} \cdot \frac{C}{C_s})} \tag{2-7}$$

Where, K_{BET} is BET equilibrium adsorption constant.

Many building materials show different adsorption and desorption isotherms. That is because in addition to the ambient conditions, the equilibrium moisture content also depends on the material initial moisture conditions or the history of drying and wetting of the materials. Although with the varying degrees, the equilibrium moisture content obtained by adsorption when the material is initially dry is always less than that obtained by desorption at the same ambient conditions when the material is initial wet, except at 0% and 100% relative humidity. This phenomenon is known as moisture Hysteresis effect (Molenda *et al.*, 1992), as shown in Figure 2-3.

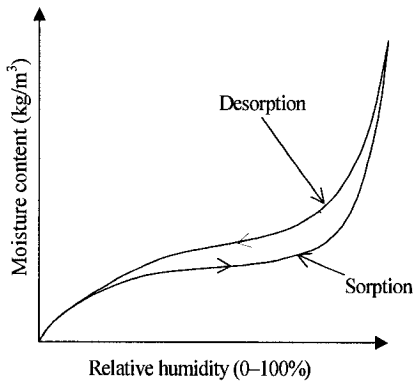

Figure 2-3 Hysteresis effect (from Molenda *et al.*, 1992)

A possible reason for such behavior is called the "Rain-drop" effect. It refers to the difference between advancing and receding contact angles, as shown in Figure 2-4, which result in different levels of moisture gain by materials (Adamson, 1990). Another explanation for this phenomenon is that in adsorption, water vapor can find its way to all pores where it may condense. While desorption is supposed to be a process of displacement by a non-wetting phase (i.e. air), but a pore may not be able to desorb its

water content. This phenomenon is called the "Ink-bottle" effect (Quenard and Sallee, 1991).

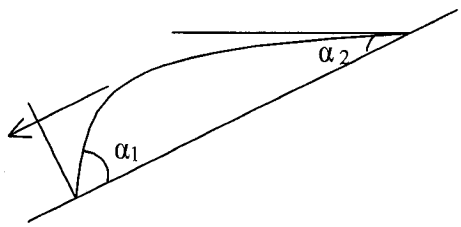

Figure 2-4 Rain-drop effect (from Adamson, 1990)

The moisture adsorption and desorption curves for many building materials have been evaluated (Pederson, 1990; Kumaran, Annex24). For most building materials, the hysterisis effect is not significant or could be simply replaced by an average of sorption and desorption curve (Pederson, 1990).

2.3.2 Review of indoor air humidity simulation models, taking into account moisture adsorption / desorption

Moisture adsorption and desorption by materials may play an important role in determining indoor air humidity behavior in buildings. Currently, most of existing indoor humidity evaluation models were strictly based on the mass balance between humidity generation rate and humidity dilution by air leakage, ignoring the moisture adsorption and desorption by interior surfaces. This could lead to considerable inaccuracy in the predicted indoor humidity level. According to Tsuchiya (1980), approximately one third

of moisture generated in a room is absorbed by its surfaces. The moisture adsorption and desorption taking place in most buildings are dynamic and alternating processes, depending on the level and the variation behavior of indoor humidity.

Both experimental and theoretical approaches have been used in studying the combined heat and moisture transport characteristics in buildings. The importance of taking into account the moisture adsorption and desorption by building materials in building simulations is also emphasized in many sources.

2.3.2.1 Experimental studies

In his indoor humidity calculation model, Kusuda (1983) suggests a method to calculate the amount of moisture adsorption by room surfaces, in which the author speculats that moisture adsorption and desorption is limited to a thin film of material (except the glass window) that attained instantaneous moisture equilibrium. In his model two parameters, the surface mass transfer coefficient and the room surface average moisture content, must be determined experimentally in order to fit the measured indoor humidity in a particular enclosure to the indoor humidity predictions. Therefore, these values may not be universally applicable for all situations. However, it has been suggested by Kusuda (1983), that the mass transfer coefficient may be approximated by a well-known Lewis relationship. To evaluate moisture conditions and transfer dynamics at the room surface, Kusuda and Miki (1985) have conducted tests at certain ambient conditions using the infrared reflectance technique called the "Quadra-Beam" method. These surface moisture

condition results can be directly implemented in the moisture adsorption model described by Kusuda (1983) as inputs; therefore, the amount of moisture absorbed or desorbed by building materials can be calculated without resorting to unknown values of the average surface moisture content. However, this requires an extensive experimental effort since the moisture conditions of each material must be evaluated at different ambient humidity levels.

Another extensive experimental study is conducted by Martin and Verschoor (1986) to investigate the cyclical moisture adsorption and desorption of fifteen materials in order to evaluate their latent heat storage effect on cooling energy consumption. The moisture response of most materials has been shown to follow exponential decay behavior. However, experimental evaluation of moisture adsorption and desorption rates at all possible initial and boundary conditions is an extremely difficult and impractical task.

Due to experimental methods having many conditional limitations and time consuming, numerical models are more practical.

2.3.2.2 Numerical models

Normally, current numerical models considering the moisture adsorption/ desorption can be classified into two main groups, i.e., the lumped and the distributed models. The typical lumped model is one of the techniques used to aid in the understanding of the moisture performance of structures. In this approach some aspects of the physical

situation to be modeled are simplified partly for this reason, but also, importantly, to provide physical insights by the introduction of concepts that have physical meaning and which aid in the understanding of the details of moisture transfer in complex systems. Compared to lumped models, the distributed models provide the range of their applications, so they are ready to be used in practical engineering design. Most commercial software belongs to this field.

2.3.2.2.1 Lumped models

One of the typical lumped models is the Effective Moisture Penetration Depth (EMPD) theory (Keresteciogl*u et al.,* 1990; Cunningham, 1992), which matches the experimental or detailed theoretical moisture adsorption and desorption rate to a simple theoretical model. EMPD is an imaginary depth, within which the moisture distribution is uniform and discontinuous between the inner regions and this thin layer of this depth. It behaves dynamically through releasing and absorbing moisture to and from the environment. For a given material, if the density, sorption isotherm, and surface area are known, the only parameter needed to know is the value of EMPD. The predictions show that indoor conditions and associated loads are very sensitive to the value of EMPD, which means ignoring moisture transport in building materials can lead to errors in load and indoor relative humidity predictions. Different EMPD values may be required for different operating conditions, and these values can be determined from experiments or detailed simulations.

In Cunningham's (1992) approach, an effective material thickness is assumed to represent the moisture transfer resistance. It is found that the effective depth for one-side exposure is a function of the angular frequency of the moisture content for a driving potential as well as the material diffusion coefficient.

$$d = \sqrt{\frac{D}{2\omega}} \qquad (2\text{-}8)$$

Where,

d : effective penetration depth, m

D : material moisture diffusivity, m^2/s

ω : angular frequency, s^{-1}

On the other hand, the effective depth for two-side exposure is found to be equal to $1/6$ of the material thickness.

However, this approach is not practical in terms of the effort needed to establish the effective moisture penetration thickness, because the material long-term moisture performances (when the inner regions of the material are affected) cannot be determined by a single value of EMPD. The concept must be used with caution and good judgment and must be backed by experimental data or detailed simulation to determine the range of applicability.

2.3.2.2.2 Distributed models

Unlike EMPD theory, Keresteciogl u and Gu (1990) presents a set of spatially distributed equations for modeling detailed heat and moisture transport in building envelope, which is called the "Evaporation and Condensation" theory. The simulation results show that the amount of moisture adsorption and desorption by building materials is significant, and temperature effect on moisture transfer is also very important. The combined heat and moisture transfer equations for building envelope are solved by the finite element method, which predicts the temperature and moisture gradients in building solids for limited case. However, "Evaporation and Condensation" theory must be verified with experiments because different types of materials have different characteristics; in addition, the sorption curve and transport coefficients for different materials are required as model inputs.

Another dynamic model of moisture adsorption and desorption by materials in the hygroscopic range is developed by El Diasty *et al.* (1993). In this model, the Biot number, *Bi*, which is defined as the ratio between the material moisture resistance to the convective mass transfer resistance, Equation (2-9) is adopted to classify materials into three main categories for determining the moisture behavior of the material within the indoor environment.

$$B_i = \frac{h_m V_m / A_e}{\delta_v} \qquad (2\text{-}9)$$

Where,

h_m : mass transfer coefficient, m/s

V_m : material volume, m^3

A_e : exposed area, m^2

δ_v : vapor permeability in materials, m^2 / s

At high Biot number ($Bi \rightarrow \infty$), the material surface attains instantaneous moisture equilibrium with the surroundings. At low Biot number ($Bi \rightarrow 0$), the material moisture behavior can be described through a lumped-parameter modeling. For most cases ($0 << Bi << \infty$), the authors believes that moisture interactions with surroundings occurre through a thin layer of material surface, and the moisture distribution is uniform and discontinuous between the inner regions and this thin layer of this depth. A commonly used one-dimensional diffusion model, as shown in Equation 2-10, is used within the material interaction depth. The amount of moisture adsorption and desorption is mainly determined by the material surface moisture condition. In order to evaluate material surface conditions, the governing moisture transfer equation is solved via an approximate analytic technique (i.e. the moment method). Comparison with experimental results, numerical solutions shows satisfactory agreement with the proposed model, but this method cannot accurately model materials response to sudden changes in ambient conditions for short times.

$$\frac{\partial P_m(x,t)}{\partial t} = D \cdot \frac{\partial^2 P_m(x,t)}{\partial x^2} \qquad (2\text{-}10)$$

Where,

P_m : partial vapor pressure within materials, Pa

D : material moisture diffusivity, m^2 / s

x: distance, m

t: time, s

A numerical model is developed in order to estimate thermal comfort by Teodosiu *et al.*, (2003), which takes into account the indoor air moisture and its transport by the airflow within an enclosure. The approach is essentially based on the computational fluid dynamics (CFD) technique, using a modified $\kappa - \varepsilon$ turbulence model ("realizable" model) to predict airflow distribution within a mechanically ventilated and natural convection test room. To obtain a field description in terms of indoor air water vapor ratio, a convection-diffusion conservation equation of vapor mass fraction is added to the basic flow equations. Based on the results achieved, the model can be particularly useful in thermal comfort studies or in situations where an exact distribution of indoor air moisture is required. In this study, the thermal comfort assessment and detailed comparisons between experimental data and numerical results are given.

In an effort to simulate the dynamic behavior of indoor air humidity and temperature, Barringer and McGugan (1989) developed a simple model for moisture storage (sorption phenomena) in building materials. In this model, a new time constant is derived for the effect of moisture storage on indoor air humidity distribution. Authors reveal that the fluctuations of indoor relative humidity (generated by varying internal gains) depend on combined storage/ventilation time constant. This time constant accounts for the effect of room volume and material surface area, as well as the material physical properties. It is an empirical parameter and highly case dependent. Therefore, it is impossible to

theoretically determine the time constant, considerable effort is needed to evaluate it for one particular material configuration either experimentally or through detailed theoretical analysis.

Another mathematical model based on heat and mass transfer equations is suggested for predicting moisture sorption rates at the interior building surfaces by Thomas and Burch (1990). The model uses moisture content as the moisture transfer potential and accounts for the temperature gradient across the material and the effect of the latent heat generated by the moisture adsorption process. The resulting heat and mass transfer equations are solved numerically by the implicit finite-difference method. Although the model predictions are found to be in good agreement with the experimental results, the node spacing and the time step have to be progressively decreased until model prediction stabilizes. Theoretical results indicate that the effect of the temperature gradient and the enthalpy on the moisture transfer process is minimal.

2.3.2.3 Energy analysis models

The models reviewed above only consider moisture transfer process within materials, but moisture adsorption and desorption within heated and cooled spaces are increasingly becoming an important part of the energy analysis models. Several typical models are reviewed as following.

A detailed three-dimensional finite element model called **M**oisture **A**dsorption and **D**esorption **A**nalysis **M**ethod (**MADAM**) is developed to evaluate the moisture adsorption and desorption rates of building envelopes and internal furnishings by Fairey and Kerestecioglue (1985). This model is based on the assumption that the moisture at the material surface is in an instant equilibrium with the environment, and explicates that adsorption and desorption phenomena are driven by the convective, diffusive, and phase-change mass fluxes. Meanwhile, in this study, the amount of absorbed and desorbed moisture is determined by solving a set of heat and mass transfer equations. However, solving these equations needs information regarding several heat and mass transfer coefficients and building material physical properties, which are available only for a few materials and are difficult to evaluate. MADAM analysis of residential cooling loads in humid climates shows that moisture adsorption and desorption can have a significant effect on air-conditioning load and on indoor relative humidity.

To predict vapor content of the indoor air and latent loads in an air-conditioned environment, a time-dependent model taking into account the moisture storage capability of the walls is developed by Isetti (Isetti *et al.*, 1988). In this model, the following equation is used to describe the moisture balance in an air-conditioned space:

$$V\frac{\partial c_i}{\partial t} = G + NV(c_0 - c_i) + M \qquad (2\text{-}11)$$

Where,

G: moisture generation rate, kg/s

N: air changes, s^{-1}

V: the volume of the room, m^3

c_o : water vapor content in the air supply, kg / m^3

c_i : water vapor content in the room air, kg / m^3

M: rate of moisture absorbed on the room surfaces, kg / s

t : time, s

The analytical results indicate that for many air-conditioning applications in which relative humidity is not strictly controlled but allows to vary within the physiological limits of people's thermal comfort, improved benefits to both cooling equipment sizing and operating costs occur when latent loads computations consider the moisture storage capability of the walls (Isetti *et al.*, 1988).

As part of an energy consumption model, Miller (1984) has suggested the use of a simple resistor-capacitor electrical circuit to describe the dynamic moisture behavior of materials. In this study, two constants, similar to what Kusuda (1983) has suggested, has to be determined experimentally.

Although these models discussed above can simulate the dynamic effect of moisture adsorption and desorption by interior materials on indoor air humidity very well, they do not take into account the process of moisture transfer within building materials, which will lead to errors in load and indoor condition predictions.

2.4 Summary

Both experimental methods and mathematical models used to study moisture transport in the building materials, adsorption and desorption phenomena of building materials, and moisture transport and distribution within indoor environment have been reviewed in this chapter. The following findings can be drawn:

1. Indoor air humidity is an important environmental factor that affects the building moisture performance, indoor air quality, and energy consumption.
2. Although there are a lot of achievements in the Heat, Air, and Moisture (HAM) model in building envelope, they neglect the effect of indoor air humidity on wall moisture performance by assuming constant indoor humidity conditions.
3. Moisture adsorption/desorption by interior building materials can greatly affect indoor air humidity conditions and building energy consumption.
4. Existing moisture simulation models do not consider simultaneously both moisture transfer within the materials and adsorption/desorption process.
5. The importance of taking into account moisture adsorption and desorption by building materials in building thermal performance simulations has been emphasized in many studies; however, these models are coupled to indoor models in which room conditions are considered well-mixed (lumped-parameter model). Therefore, the non-uniform behavior distribution of the air and humidity within the room, which is important in comfort analysis and condensation study, cannot be evaluated.

From the above finding, we can see there is a need for an accurate model that could predict indoor humidity behavior and distribution within a room, and this also consolidates the importance and the potential of present study.

To fill this gap, this study presents a new modeling approach to predict indoor air humidity behavior and distribution, and it will be introduced in the next chapter.

Chapter 3

INTEGRATING BUILDING MATERIAL MOISTURE TRANSPORT MODEL WITH ZONAL MODEL

3.1 Introduction

Indoor air humidity is influenced by the characteristics of a room and its mechanical systems, such as ventilation strategies, occupant's behavior, temperature distribution, etc. A detailed knowledge of indoor air humidity distribution is important for Indoor Air Quality (IAQ) and energy consumption control. Therefore, there is a need to find an accurate and simplified method to predict transient temperature and humidity distribution within a room.

The existing methods of predicting temperature and humidity distribution in a room include experimental methods and numerical models. Experimental methods can provide high quality measurement data, but they are time-consuming and expensive. Moreover, it is difficult to get the information on the sensitivity of parameters in experimental investigations. For numerical model, the CFD model is one of the powerful tools currently available to analyze the indoor air conditions. The CFD model can provide users with the detailed knowledge of airflow pattern, temperature and contaminant distributions within a room, and it was also demonstrated to be a potential tool to predict and model time dependent humidity distribution in enclosed spaces (Nielsen, 1989); however, it is too complicated to be used as a daily design tool, including some very good

commercially available software, especially to be used by non-specialists. It is time consuming and expensive. Furthermore, for building engineering, the users are not usually interested in the excessively discredited results that can be obtained from a CFD model. Another promising numerical method for indoor parameter simulation is the zonal model, and it was first proposed by Lebrun in his Ph.D thesis in 1970 (Allard and Inard, 1992). Zonal models (Inard *et al.,* 1996; Musy, 1999) are an alternative to CFD models. In zonal models, a room is divided into a relatively small number of zones—typically on the order of tens to hundreds—compared to thousands and more for typical CFD simulations. As a result, zonal models can get results much faster than CFD calculations, and it has advantages over CFD model in its easiness to use, computationally efficiency, and time saving characteristics (Haghighat *et al.*, 2001; Axley, 2001).

Zonal models have been widely utilized in building simulations. For instance, zonal models were integrated with convection, conduction and radiation heat transfer models to predict velocity and temperature distribution within a room (Inard *et al.*, 1996; Wurtz *et al.*, 1999a; Wurtz *et al.*, 1999b and Musy *et al.*, 2001). Haghighat *et al.* (2001) and Rutman *et al.* (2002) adopted zonal model to predict thermal comfort in a room, such as PPD (Predicted Percentage of Dissatisfied). Huang and Haghighat (2002) developed an integrated zonal model to simulate the VOC (Volatile Organic Compound) concentration distribution in a ventilated room. Whereas, zonal models integrated with mass transfer models to simulate the humidity distribution within a room are seldom available. Recently, Mendonca *et al.* (2002) proposed a zonal model to demonstrate the influence of adsorption/ desorption by building materials on indoor air behavior. Simple theoretical

results were presented in this research by the object-oriented simulation environment, SPARK (Sowell and Haves, 2001). Although many achievements have been made in the development of the zonal model, a zonal model that is integrated with moisture transfer model in materials in order to predict humidity distribution in a room air is not yet available.

This chapter describes the development of an integrated zonal model for predicting the transient humidity distribution in a ventilated room, in which a zonal model is incorporated with a building material moisture transfer model.

3.2 Zonal Model

Different zonal models utilize different driving forces to distinguish themselves when modeling airflow. This study uses Huang's model (Huang, 2003) to simulation. This model uses Power Law to describe the airflow across the cell interface (Wurtz *et al.*, 1999a; Wurtz *et al.*, 1999b and Haghighat *et al.*, 2001). It describes the airflow in terms of the pressure difference and assumes that the pressure is hydrostatically distributed in a cell instead of being uniform. The general information about zonal model is simply introduced as following (Huang, 2003):

In the zonal model, the physical system is a room with mechanical ventilation system at a non-isothermal condition. The room is divided into a limited number of three-

dimensional small cells with homogeneous thermal property within each cell. The room configuration and partition are shown in Figure 3-1.

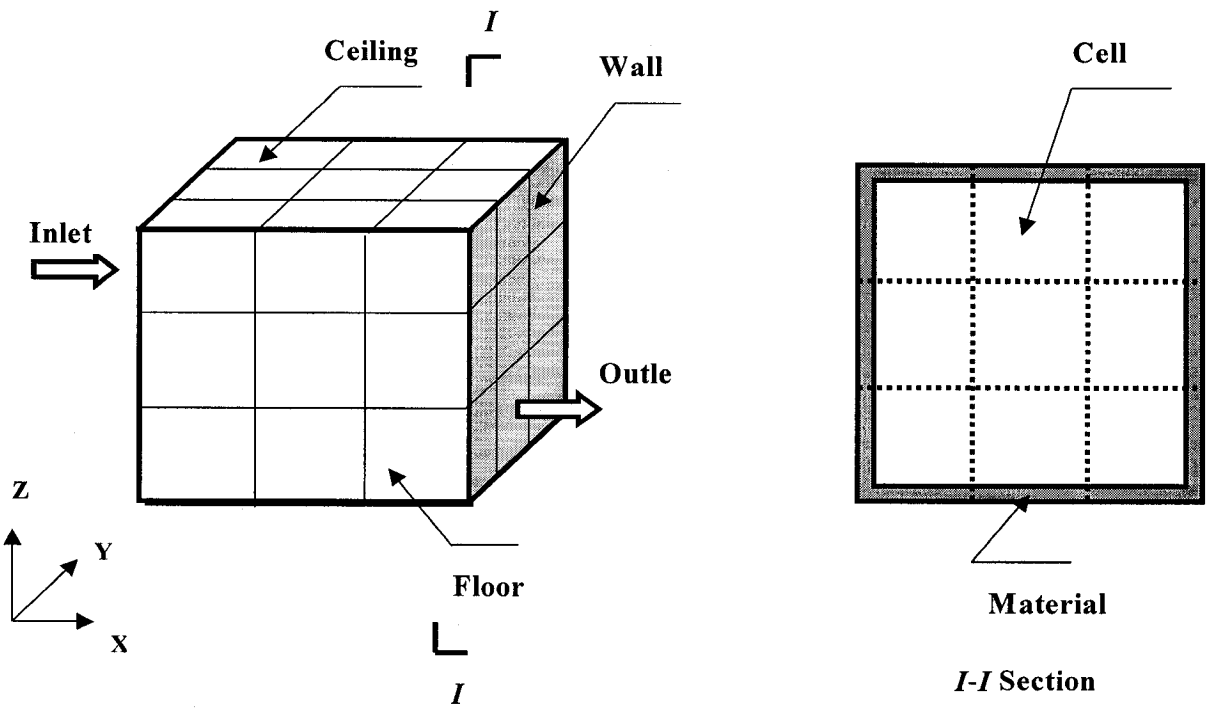

Figure 3-1 Room physical configuration and partition

3.2.1 Air mass and energy conservation equations

Within each cell, pressure at the middle of the cell is assumed to obey the Perfect Gas Law (Hutcheon and Handegord, 1989) and pressure hydrostatically varies with assuming an independent reference pressure at the bottom of each cell, as show in Equations (3-1) and (3-2).

$$P_{middle,i} = \rho_i R T_i \qquad (3\text{-}1)$$

$$P_{i,h} = P_{ref,i} - \rho_i g H \tag{3-2}$$

Where,

$P_{middle,i}$: pressure at the middle of cell i, Pa

ρ_i : air density of cell i, Kg/m^3

R : gas constant of air, 287.055 $J/kg \cdot k$, (Hutcheon and Handegord, 1989)

T_i : temperature of the cell i, K

$P_{ref,i}$: reference pressure of cell i, Pa

H : height of the cell, m

$P_{i,h}$: pressure at the height of h in cell i, Pa

g : gravitational acceleration, m^2/s

In each cell, the principle of conservation of mass and energy must be obeyed. In this study, we only consider with rooms in steady state condition, time derivatives of mass and heat in cell i are zero. Therefore, the mass and heat exchange between adjacent cells through the cell interfaces can be expressed as (Huang, 2003):

$$0 = \frac{dM_i}{dt} = \sum_{j=1}^{n} m_{ij} + m_{source} + m_{\sin k} \tag{3-3}$$

$$0 = \frac{dQ_i}{dt} = \sum_{j=1}^{n} q_{ij} + q_{source} + q_{\sin k} \tag{3-4}$$

Where,

M_i, Q_i : mass and heat in cell i, kg and J, respectively

m_{ij}, q_{ij} : mass and heat flow across cell i and cell j interface, kg/s and W, respectively

m_{source}, q_{source} : rate of mass and energy generated in cell i, kg/s and W, respectively

$m_{\sin k}, q_{\sin k}$: rate of mass and energy consumed from cell i, kg/s and W, respectively

Power law is applied to calculate airflow rate across the adjacent zones interface, as shown in Equation (3-5),

$$m_{ij} = C_d A \rho_i \Delta P_{ij}^n \qquad (3\text{-}5)$$

Where,

m_{ij} : mass flow rate across cell i and j interface, kg/s

C_d: coefficient of Power law, usually taken as 0.83, $kg/s \cdot P_a^n$ (Wurtz *et al.*, 1999a; Wurtz *et al.*, 1999b and Haghighat *et al.*, 2001)

A: area of interface, m^2

ρ_i : density of the cell, kg/m^3

ΔP_{ij} : pressure difference between cell i and j, Pa

n: flow exponent, usually taken as 0.5 (Wurtz *et al.*, 1999a; Wurtz *et al.*, 1999b and Haghighat *et al.*, 2001).

In Huang's model, the radiation component is ignored so that the heat flow is a combination of convection along wall surfaces and the heat carried by mass flow (Huang, 2003). The heat flow rate across cell i and j interface is mainly through convection and can be obtained by:

$$q_{ij} = m_{ij} C_p T \qquad (3\text{-}6)$$

if $m_{ij} > 0$,

$$q_{ij} = m_{ij} C_p T_j \tag{3-7}$$

if $m_{ij} < 0$,

$$q_{ij} = m_{ij} C_p T_i \tag{3-8}$$

And Newton cooling law is used to model heat transfer along wall surfaces. The heat flow rate along wall surface is

$$q_{ij} = h_c A \Delta T_{i-wall} \tag{3-9}$$

where,

T_i : temperature of cell i, K

T_j : temperature of cell j, K

C_p : specific heat of air, J / kgk

h_c : convective heat transfer coefficient, $W / m^2 K$

ΔT_{i-wall} : temperature difference between cell i and wall, K

A: area of interface between cell i and wall, m^2

3.2.2 Boundary Conditions

3.2.2.1 Airflow across horizontal boundary

The airflow across the horizontal boundary between two adjacent cells can be modeled by Power Law, like Equation (3-5). The physical configuration is shown in Figure 3-2.

In this study, the pressure at the bottom level of the zone is assumed to be uniform and can be expressed as reference pressure, $P_{ref,i}$. The airflow rate can be calculated as (Haghighat *et al.*, 2001):

$$m_{ij,hor} = C_d A \rho_i (P_{ref,i+1} - P_{ref,i} + \rho_i g H)^n \qquad (3\text{-}10)$$

Where,

$m_{ij,hor}$: airflow rate across horizontal boundary, kg/s

P_{ref}: reference pressure of the cell i and i+1, respectively, Pa

H: height of the cell i, m

ρ_i: density of the cell i, kg/m^3

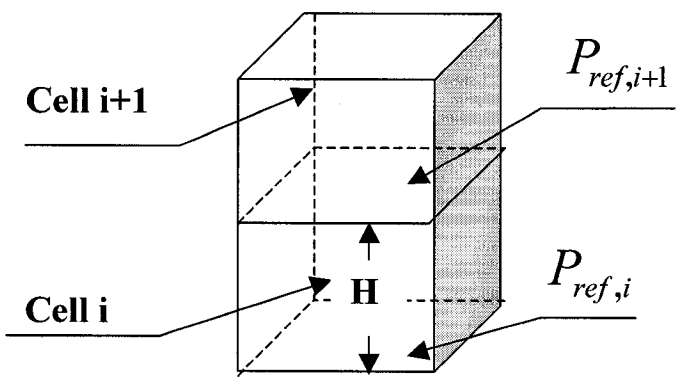

Figure 3-2 Physical configurations for modeling horizontal boundary

When the pressure above the horizontal boundary is larger than that below the boundary, i.e.

$P_{ref,i+1} - p_{ref,i} + \rho_i g H \geq 0$, the airflow rate is

$$m_{ij,hor} = -C_d A \rho_{i+1} \left| P_{ref,i+1} - P_{ref,i} + \rho_i g H \right|^n \qquad (3\text{-}11)$$

When the pressure above the horizontal boundary is less than that under the boundary, i.e.

$P_{ref,i+1} - p_{ref,i} + \rho_i g H < 0$, the airflow rate is

$$m_{ij,hor} = C_d A \rho_i \left| P_{ref,i+1} - P_{ref,i} + \rho_i g H \right|^n \qquad (3\text{-}12)$$

3.2.2.2 Airflow across vertical boundary

For calculating airflow across vertical boundary, a neutral plane (Z_n) is assumed. At the height of which the pressure difference between both sides of the vertical boundary is zero (Haghighat *et al.*, 2001). The physical configuration is shown in Figure 3-3.

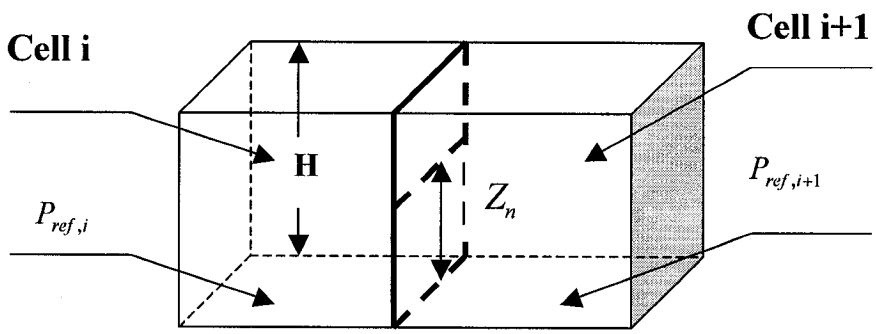

Figure 3-3 Physical configurations for modeling vertical boundary

Therefore, at the height of the neutral plane, the pressure difference between cell i and i+1 is zero,

$$\Delta P_{ref} - \Delta\rho g Z_n = 0 \tag{3-13}$$

$$Z_n = \frac{\Delta P_{ref}}{\Delta\rho g} \tag{3-14}$$

Where,

ΔP_{ref} : difference of the reference pressure between the cell i and i+1, Pa

$\Delta\rho$: difference of the density between the cell i and i+1, kg/m^3

Z_n : the height of the neutral plane, m

Thus, as shown in Figure 3-3, the total airflow rate across vertical boundary can be expressed as:

$$m_{ver} = m_{0-Z_n} + m_{Z_n-H} \tag{3-15}$$

Where,

m_{0-Z_n} : airflow rate under neutral plane, kg/s

m_{Z_n-H} : airflow rate above neutral plane, kg/s

m_{ver} : total airflow rate across vertical boundary, kg/s

Then, substituting Equations (3-5) and (3-14) into Equation (3-15), the total airflow rate across vertical boundary becomes:

If $\rho_i > \rho_{i+1}$,

$$m_{ver} = C_d A \rho_i \left|\Delta\rho g\right|^n \frac{\left|Z_n\right|^{n+1}}{n+1} - C_d A \rho_{i+1} \left|\Delta\rho g\right|^n \frac{\left|H - Z_n\right|^{n+1}}{n+1} \tag{3-16}$$

If $\rho_i < \rho_{i+1}$,

$$m_{ver} = -C_d A \rho_{i+1} \left|\Delta \rho g\right|^n \frac{\left|Z_n\right|^{n+1}}{n+1} + C_d A \rho_i \left|\Delta \rho g\right|^n \frac{\left|H - Z_n\right|^{n+1}}{n+1} \quad (3\text{-}17)$$

If $\rho_i = \rho_{i+1}$, $P_{ref,i} \geq P_{ref,i+1}$,

$$m_{ver} = C_d A \rho_i \left|P_{ref,i} - P_{ref,i+1}\right|^n \quad (3\text{-}18)$$

If $\rho_i = \rho_{i+1}$, $P_{ref,i} < P_{ref,i+1}$,

$$m_{ver} = -C_d A \rho_i \left|P_{ref,i} - P_{ref,i+1}\right|^n \quad (3\text{-}19)$$

3.3 Integrating Building Material Moisture Transport Model with Zonal Model

Most building materials such as concrete, wood, gypsum, and brick products can be considered as porous materials (Blondeau *et al.*, 2000). The proposed model is developed for porous materials that have an effective diffusion coefficient. The building material considered here is treated as a porous medium. The moisture transports through material first by internal diffusion to the material surface; over material surface, there is a mass boundary layer, water vapor transfer in this boundary is through diffusion and convection; then followed this boundary layer water vapor transfer to the bulk air by diffusion and convection. Water vapor transfer from the material to the air follows the following three main processes, as shown in Figure 3-4.

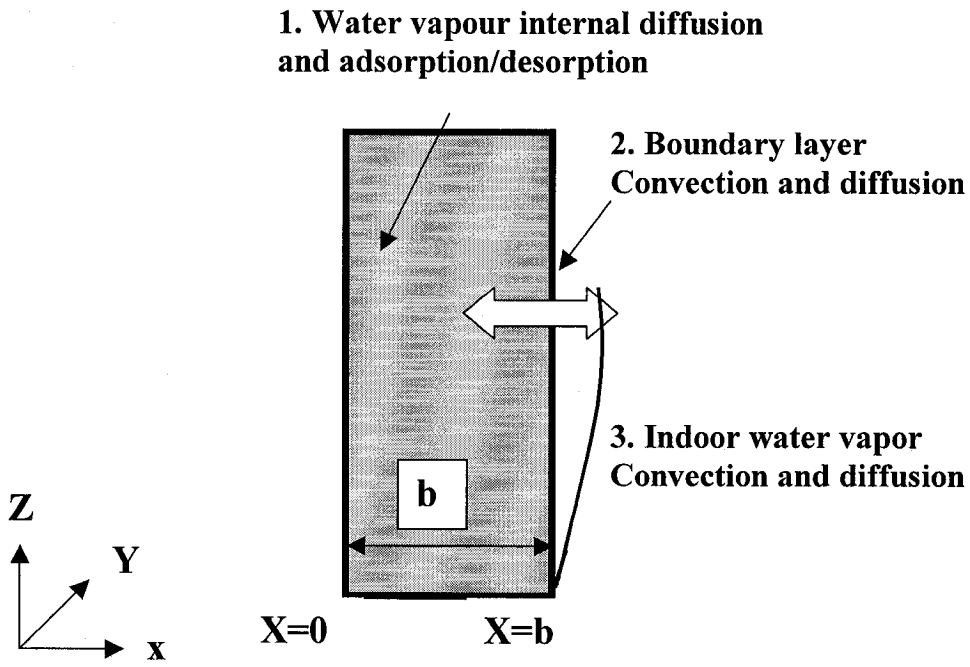

Figure 3-4 Schematic diagram of the model description

3.3.1 Moisture transfer within the materials

The dynamic moisture transfer process within a porous material is a complex phenomenon with vapor diffusion, capillary forces, and evaporation-condensation, etc. Moisture exists in gas-phase and adsorbed-phase within the pores and internal diffusion is assumed as the main transfer mechanisms as reviewed in Chapter 2. The amount of moisture transfer mainly depends on the surface moisture condition, as well as the surface mass transfer coefficient. In the development of moisture transfer model, the following assumptions are made:

- Water vapor density (or partial vapor pressure) is the only driving force;
- The problem is isothermal, i.e. heat generated by moisture sorption is assumed negligible;

- Hysteresis effect is negligible.

With these assumptions, three-dimensional water vapor transmission through a porous material may be described as:

$$\frac{\partial \rho_m}{\partial t} = \frac{\partial}{\partial x}(D\frac{\partial \rho_m}{\partial x}) + \frac{\partial}{\partial y}(D\frac{\partial \rho_m}{\partial y}) + \frac{\partial}{\partial z}(D\frac{\partial \rho_m}{\partial z}) \qquad (3\text{-}20)$$

Where,

$$D = \frac{D_v}{\rho \cdot C_m} \qquad (3\text{-}21)$$

ρ_m : water vapor density in the materials, kg/m^3

x, y, z : distance in different directions, m

D : material moisture diffusivity, m^2/s

D_v : vapor permeability, $kg/m \cdot Pa \cdot s$

C_m : material moisture capacity, $kg/kg \cdot Pa$

ρ : material density, kg/m^3

3.3.2 Moisture transfer in boundary layer

Moisture adsorption and desorption taking place in most buildings are dynamic and alternating processes depending on the surface moisture condition of the materials and the various behaviours of the indoor humidity. When moisture content at the material surface is higher than moisture content in the surrounding air, moisture will transport to the surrounding air. When moisture content at the material surface is lower than moisture

content in the surrounding air, moisture will be adsorpted by materials. In this study, as most common practice, moisture transfer at the material surface is treated as convection; therefore, the third boundary condition can be used to describe the convection mass transfer. In the boundary layer, mass transfer rate is equal to the moisture adsorption/ desorption rate.

$$-\delta_v \frac{\partial \rho_m(x,t)}{\partial x} = h_m[\rho_m(b,t) - \rho_{wv}] \qquad \text{at} \quad x = b \qquad (3\text{-}22)$$

Where,

δ_v : water vapor permeability in the material, m^2 / s

The driving force for mass transfer process in the boundary layer is the difference between water vapour density at the material surface and that of the indoor air. The rate of moisture transfer at the material /air interface can be written as the following Equation:

$$m_{wv} = Ah_m[\rho_m(b,t) - \rho_{wv}(t)] \qquad (3\text{-}23)$$

where,

m_{wv} : moisture adsorption/desorption rate, kg / s

A : mass transfer area of interface, m^2

h_m : convection mass transfer coefficient, m / s

ρ_m : water vapor density of material, kg / m^3

ρ_{wv} : water vapor density in the cell air, kg / m^3

3.3.3 Mass balance in the room

The water vapor is transported in the room air through convection and diffusion, assuming that the moist air in a zone is well mixed. The transient water vapor balance equation can be expressed by:

$$v\frac{d\rho_{wv}}{dt} = \sum_{i=1}^{6} m_{wv} + m_{wv,source} + m_{wv,\sin k} \qquad (3\text{-}24)$$

Where,

i : refer to face i of the cell

ρ_{wv} : water vapor density, kg/m^3

m_{wv} : water vapor mass flow rate, kg/s

$m_{wv,source}$: water vapor source, kg/s

$m_{wv,\sin k}$: water vapor sink, kg/s

v : the volume of the cell, m^3

t : time, s

The water vapor flow cross both vertical and horizontal interfaces of cells includes a diffusion term and a convection term due to pressure difference between adjacent cells. The water vapor flow due to pressure difference between adjacent cells is determined by dry-air flow, as equation,

$$P_{ma,i} \geq P_{ma,i+1}, \qquad m_{wv} = m_{ij}\frac{\rho_{wv,i}}{\rho_i} \qquad (3\text{-}25)$$

$$P_{ma,i} \leq P_{ma,i+1}, \qquad m_{wv} = m_{ij}\frac{\rho_{wv,i+1}}{\rho_{i+1}} \qquad (3\text{-}26)$$

$$P_{ma,i} = (\rho_i R_{da} + \rho_{wv} R_{wv}) T_i \qquad (3\text{-}27)$$

Where,

$P_{ma,i}$: total pressure of moist air in the cell i, Pa

The water vapor flow by diffusion is calculated by Fick's Law,

$$m_{wv} = D_a \cdot A \cdot \left(\frac{\rho_{wv,i} - \rho_{wv,i+1}}{\frac{l_i + l_{i+1}}{2}} \right) \qquad (3\text{-}28)$$

Where,

l: cell's dimension perpendicular to the interface, m

The Hybrid Scheme developed by Spalding (1972) is used to calculate the mass flux of water vapor density across interface by diffusion and convection.

3.3.4 Initial and boundary conditions

Some initial conditions and boundary conditions are needed to close the above equations.

a) Initial conditions:

A homogeneous material in the hygroscopic range is assumed with an initial water vapor density:

$$\rho_m(x, y, z, 0) = \rho_{m0} \qquad \text{at} \quad t = 0 \qquad (3\text{-}29)$$

In the room air, the initial water vapor density is the moisture background density:

$$\rho_{wv}(0) = \rho_{wv0} \tag{3-30}$$

The water vapor density in the supply air is described as:

$$\rho_{\sup ply} = \rho_{in} \tag{3-31}$$

Where,

ρ_{m0} : initial water vapor density in the material, kg/m^3

ρ_{wv0} : initial water vapor density in the room air, kg/m^3

ρ_{in} : water vapor density in the inlet air, kg/m^3

$\rho_{\sup ply}$: water vapor density in the supply air, kg/m^3

b) Boundary conditions

The third boundary condition can be used to describe the convective mass transfer. At the material and air interface, mass transfer rate is equal to the moisture adsorption/ desorption rate.

$$-\delta_v \frac{\partial \rho_m(x,t)}{\partial x} = h_m[\rho_m(b,t) - \rho_{wv}] \qquad \text{at} \quad x = b \tag{3-32}$$

It is assumed that there is no moisture passing through the bottom surface of the material,

$$-\delta_v \frac{\partial \rho_m}{\partial x} = 0 \qquad \text{at} \quad x = 0 \tag{3-33}$$

3.3.5 Parameter estimation

There are four parameters that need to be determined: the mass transfer coefficient in the air, h_m; moisture diffusivity in the material, D_m; water vapor diffusivity in the room air, D_a; water vapor permeability in the material, δ_v.

3.3.5.1. Mass transfer coefficient in the air, h_m

Since the mass transfer coefficient in the air, h_m, is not as sensitive to room characteristics as other parameters (Kusuda, 1983), an approximate theoretical relationship, such as well known Lewis relationship, can be used to evaluate it. Lewis relationship is given in Equation (3-34):

$$h_m = \frac{h_c}{\rho_a C_p} \tag{3-34}$$

Where,

C_p: air specific heat, $J/kg \cdot k$

h_c: convective heat transfer coefficient, $w/m^2 \cdot k$

In the building indoor environment, the value of the convective heat transfer coefficient, h_c, is either determined by the natural convective process or the airflow pattern within the space. According to Kusuda (1983), an average surface convective heat transfer coefficient of about $0.00068\,m/s$ can be used in evaluating the mass transfer coefficient within indoor environment.

The magnitude of the convective heat transfer coefficient, h_c, can be calculated as forced convection heat transfer coefficient. There are several methods to calculate it.

1. The surfaces of the building envelope are flat surfaces. When a mechanical ventilation system is operating, the air will flow over the inside surfaces of various building envelop, such as walls, windows, ceilings and floors. Hence, during operating periods, a forced convective heat transfer occurs.

For forced convection, even at an air velocity V= 0.5 m/s and the length of the flat plate L=3.6m, the Reynolds number of the fluid flow at the surface of the building envelope is:

$$\mathrm{Re}_L = \frac{vL}{\gamma} = \frac{0.5 \times 3.6}{1.62 \times 10^{-5}} = 1.11 \times 10^5 \leq 5 \times 10^5 \qquad (3\text{-}35)$$

Hence, the fluid flow is laminar. Then, for a flat plate in laminar flow, the relation is

$$Nu = 0.664\,\mathbf{Re}^{1/2}\,\mathbf{Pr}^{1/3} \qquad (3\text{-}36)$$

$$h_c = \frac{k}{L} Nu \qquad (3\text{-}37)$$

$$\mathbf{Pr} = \frac{\gamma\, C_p}{k} \qquad (3\text{-}38)$$

Where,

k : Thermal conductivity, $w/m \cdot k$

γ : viscosity, $kg/m \cdot s$

2. ASHRAE Fundamentals (2001) recommends a simplified empirical formula developed by McAdams for evaluation of the convective heat transfer coefficient of vertical planes when the air velocity flows over the surface at $v \leq 5 m/s$,

$$h_c = 5.6 + 3.9v \tag{3-39}$$

3. According to Wurtz (1999), for natural convection, the convective heat transfer coefficient depends on the surface-to-air temperature difference according to:

$$h_c = C(T_i - T_{w,i})^n \tag{3-40}$$

For which the values of the coefficient C and n are given in the Table 3.1.

Table 3.1 Values of Coefficient C and Exponent n in the expression for convective heat transfer coefficient (from Wurtz, 1999)

		c	n	Reference
Ceiling	Natural convection	3	0	Allard, 1987
	Mixed convection	3	0.7	Inard, 1988
Roof	Heated ceiling	1.5	1/3	Kast and Klan, 1982
	Other cases	3	0	Allard, 1987
Walls	Natural convection	1.5	1/3	Allard, 1987
	Mixed convection	3	1/3	Lebrun, 1970
	Plume at face	0.662	0.77	Inard, 1988

3.3.5.2 Moisture diffusivity in the building material, D_m

The material physical properties required for modeling moisture transfer depend on which moisture potentials are used. When water vapor density (or partial vapor pressure) is used as the main driving force, the water vapor diffusivity, D_m, will be required for modeling moisture transfer. Moisture diffusivity of the material is usually a function of many factors, such as pore structure, material type, compound properties, temperature, and moisture content. The dependence of the water vapor diffusion coefficient on moisture content has been evaluated for some materials (Annex24, 1996); and it can be summarized by Equation (3-41):

$$D_w = C_1 \exp(C_2 w) \qquad (3\text{-}41)$$

Where, w is moisture content, kg/m^3, and values of the coefficients C_1 and C_2 are given in Table 3-2 for different building materials (Annex24, 1996).

3.3.5.3 Water vapor diffusivity in the room air, D_a

According to Sherwood and Pigford (1952), the molecular diffusivity of water vapor in air is given by the following equation (valid up to 1366K):

$$D_a = (9.26 \times 10^{-4} / P) T^{2.5} / (T + 245) \qquad (3\text{-}42)$$

Where,

P: total pressure, Pa

T: temperature, K.

Table 3-2 Values of coefficients C_1 and C_2 for evaluating of water vapour diffusion coefficients from different building materials

Material	$C_1 \times 10^{-10}$	$C_2 \times 10^{-2}$
Concrete	0.18	5.82
Lightweight Concrete	13	3.51
Aerated Concrete	0.92	2.15
Brick	21	3.16
Cement Mortar	20	2.2
Plywood	0.0032	1.5
Polystyrene Concrete	4.6	6.4

3.3.5.4 Water vapor permeability in the material, δ_v

The vapor permeability at a point is defined as the ratio between the density of vapor flow rate at that point and the magnitude of the vapor concentration gradient in the direction of the flow. The definition for vapor permeability stems from the transport equation (Annex 24, 1996):

$$m_v = -\delta_v grad\rho_v \qquad (3\text{-}43)$$

Among all the moisture transport properties, the vapor permeability of building materials are most readily measurable and also received considerable attention in the past few years. Galbraith et al. (1992) reported the comparability of water vapor permeability measurements. The simplest method of finding the permeability of a specimen is the cup method, including the dry-cup method and wet-cup method (ASHRAE Fundamental,

2001). That is to seal a specimen over the top of a cup containing either a desiccant or water, place it in a controlled atmosphere, and weight it periodically. The steady state of weight gain and loss will give the water vapor transfer from which the permeability can be calculated. Various data reported in the literature show that for most of the hygroscopic materials, the vapor permeability is a strong function of the mean relative humidity of the material.

3.4 Solution Techniques

3.4.1 Newton-Raphson Global Convergence Technique

The steady state indoor air flow pattern analysis for zonal model needs the simultaneous solution of mass and energy balance equations (3-3 and 4) for all zones. Since Power Law, the functions of mass balance equations are non-linear; therefore, a method for solving non-linear algebraic equations is required.

Lin (1999) and Huang (2003) demonstrated that Newton-Raphson global convergence (Press, 1992) technique has been demonstrated that it is a suitable numerical technique for solving the present non-linear systems. Newton-Raphson method is a root finding method of a function and can be used to solve the non-linear problem by an iteration of the solutions of linear equations. To be simplified, Newton-Raphson method can be explained as follow. For a problem gives N functional relations involving N variables to be zero:

$$F_i(x_i) = 0 \qquad \text{i=1,2,.....N} \qquad (3\text{-}44)$$

By using a guess value, the functional and first order derivative value can be gotten. Plotting a straight tangential line using the derivative as slope, then get a new root value on the X axis. Redo the above procedure, using the new root value until the root value converged. More detail express about Newton-Raphson method can be found in Press *et al.* (1996). In this study, Newton Raphson global convergence technique is applied to solve a set of coupled nonlinear mass and linear heat equations to get the air flow crossing each cell interface. The airflow across each cell interface is directly used in humidity mass balance equation as input.

3.4.2 Combined TDMA and Gauss-Seidel method

To solve the set of humidity mass balance equations to get humidity distribution in the room and materials, a combination of the Tri-Diagonal-Matrix-Algorithm (TDMA) and the Gauss-Seidel method, named line-by-line method (Patankar, 1980) is applied. The Gauss-Seidel method is a technique for solving the linear system of equations--- one at a time in sequence and uses previously computed results as soon as they are available. The details can be seen in Appendix I.

3.5 Model validation

Moisture adsorption and desorption by materials is a very complex moisture transfer process to model because of the moisture coupling which exists both in the indoor air and the building material. The proposed model for evaluating the surface moisture conditions

of the material is firstly compared with Kusuda and Miki's experimental results (Kusuda and Miki, 1985) and El Diasty's theoretical results (El Diasty *et al.,* 1993) of an adsorption test on a $3\,mm$ thick balsa wood specimen. The specimen is exposed to constant ambient conditions of 24°C and 70% relative humidity from both sides, thus half the specimen's thickness ($1.5\,mm$) is theoretically modeled. For balsa wood, a density of $160\,kg/m^3$, the moisture adsorption isotherm curve and all input parameters, as shown in Figure 3-5 and in Table 3-1, are taken from literatures. Although it is an important parameter in the modeling process, the value of mass transfer coefficient, h_m, in Kusuda and Miki's experiment (1985), is not known and can not be evaluated using Lewis relationship; however, according to Kusuda (1983), an average value 0.00068 m/s is used in the case.

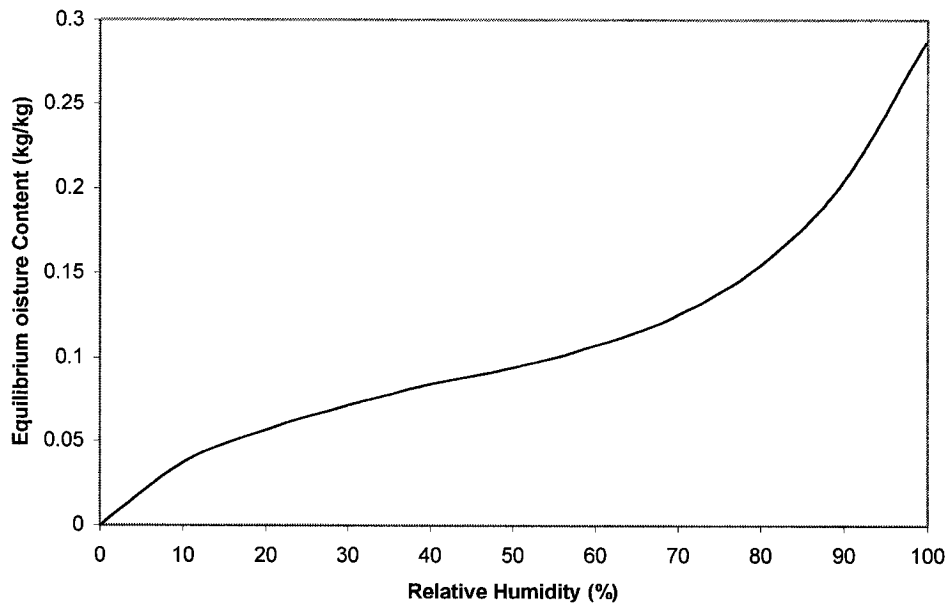

Figure 3-5 Wood moisture adsorption isotherms (from Keresteciogiu, 1990)

Table 3-3 Values of the input parameters for validation (I)

Parameter	ρ_{wv0}	ρ_{m0}	D_m	D_a	δ_v	h_m
(unit)	kg/m^3	kg/m^3	m^2/s	m^2/s	m^2/s	m/s
Value	0.015	0.0015	1.0×10^{-10}	2.63×10^{-5}	1.31×10^{-7}	0.00068

Figure 3-6 shows the comparison of the prediction results by the proposed model with experimental results (Kusuda and Miki, 1985) and theoretical evaluation results (El Diasty *et al.,* 1993) of the transient behavior of the surface moisture conditions of the balsa wood specimen. It can be seen that there is a good agreement between the proposed model and the El Diasty's model; in addition, a better agreement can be obtained when smaller surface mass transfer coefficients are used, since the theoretical curve will be shifted downward (El Diasty *et al.,* 1993).

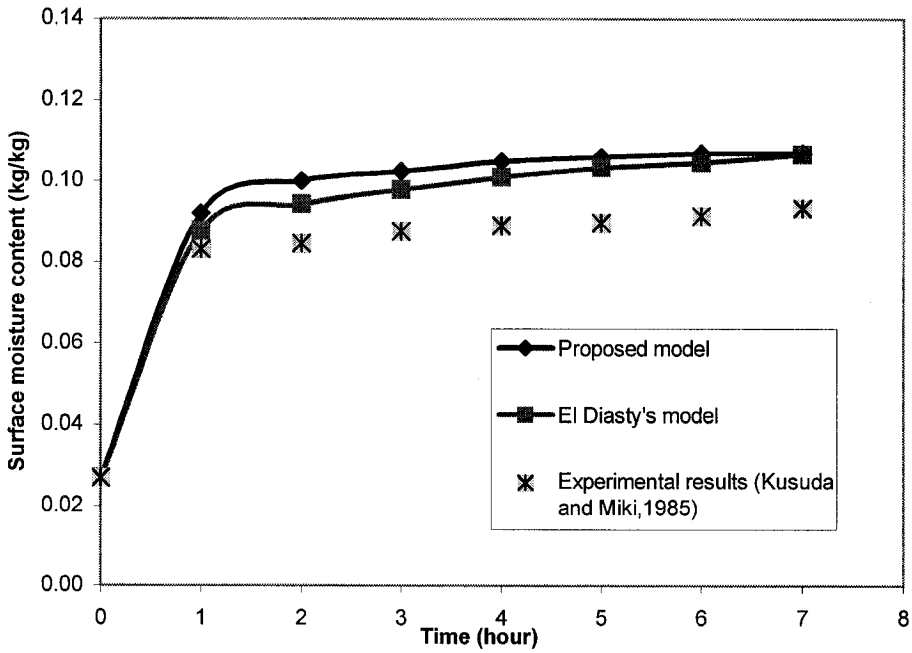

Figure 3-6 Comparison of prediction results of surface moisture content with literature data

In addition, the results of the proposed model are also compared with the experimental results of a desorption test on a 13 mm thick gypsum board specimen (Thomas and Burch, 1990). In this experimental test, material moisture and physical characteristics and initial condition were clearly defined, as shown in Table 3-4. The moisture capacity of the gypsum board was modeled by the moisture adsorption isotherm, as shown in Figure 3-7.

Table 3-4 Values of the input parameters for validation (II)

Parameter	ρ_{wv0}	ρ_{m0}	D_m	D_a	δ_v	h_m
(unit)	kg/m^3	kg/m^3	m^2/s	m^2/s	m^2/s	m/s
Value	0.0057	0.016	1.8×10^{-8}	2.63×10^{-5}	6.21×10^{-6}	0.0044

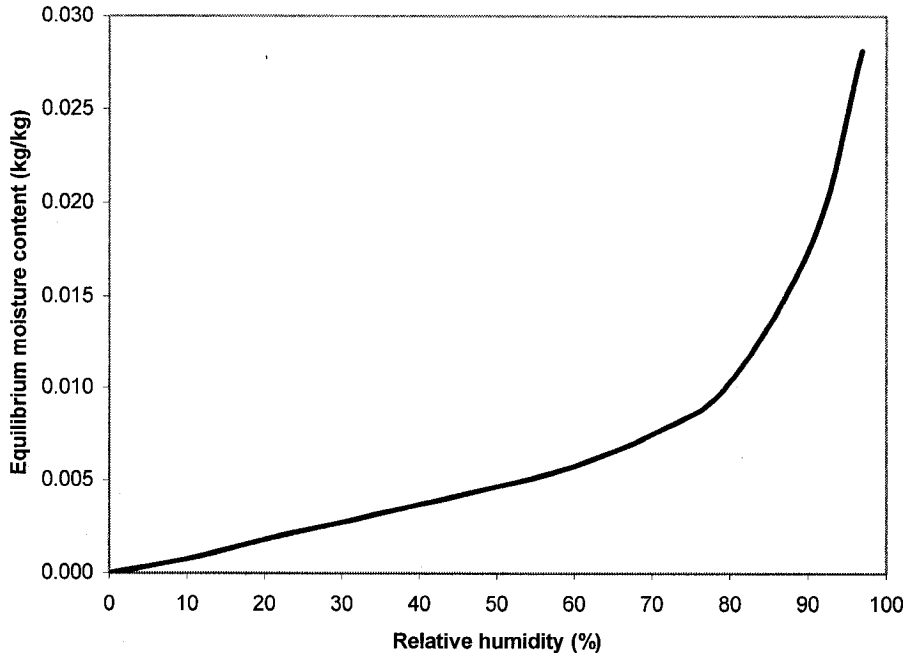

Figure 3-7 Gypsum board moisture adsorption isotherms (from Thomas and Burch, 1990)

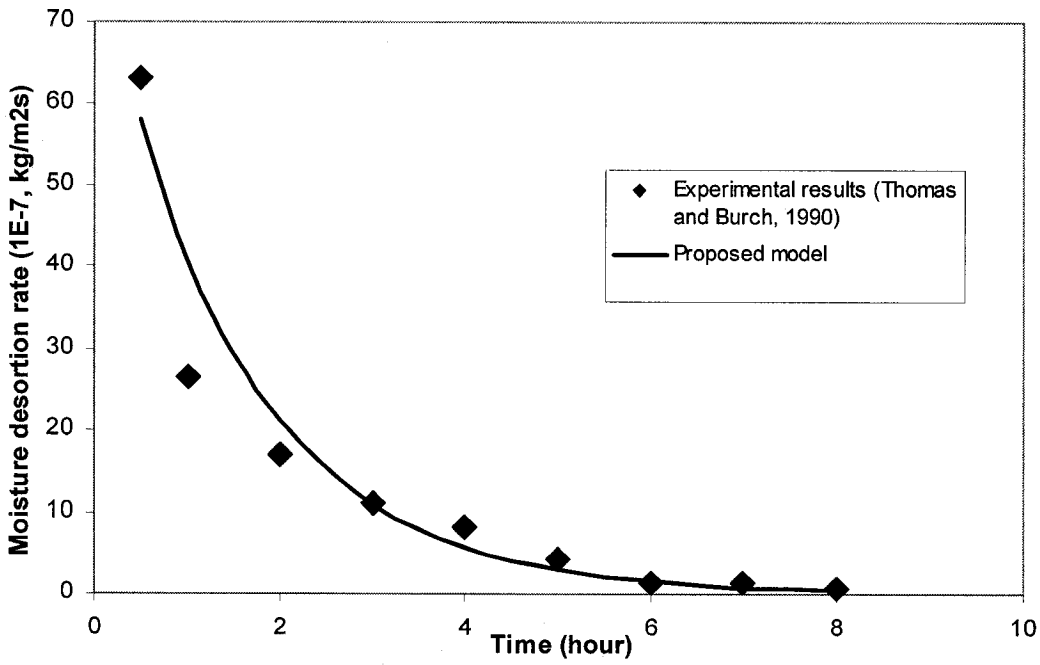

Figure 3-8 Comparison between experimental results and theoretical prediction of moisture desorption rates

Experimental and theoretical evaluations of moisture desorption rates of the gypsum board specimen are shown in Figure 3-8. It can be seen that the predicted result is in satisfactory agreement except at the beginning of the process. This can be attributed to measurement uncertainties at the beginning of the experiment and the sensitivity of the mass balance scale used (Thomas and Burch, 1990).

3.6 Case study

After the proposed model has been validated with the experimental data and the theoretical results in the literatures, it is demonstrated that the proposed model could accurately model the dynamic effect of moisture adsorption and desorption by interior materials. Furthermore, the proposed model has been applied in three cases to investigate the practicality in their general applications.

3.6.1 Case 1: Non-ventilation

To investigate the impact of material moisture adsorption/ desorption on indoor humidity distribution, the proposed model is firstly applied to a non-ventilated room. In this case, the physical configuration is adopted as one of the MINIBAT tests (CETHIL – INSA de Lyon, France) (Inard *et al.*, 1996). The installation is an identical enclosure ($3.10 \times 3.10 \times 2.50 m^3$) and in a non-isothermal condition. The temperature and the heat transfer coefficients of exterior walls are shown in Table 3-5. It is assumed that the east, west, south, north wall and ceiling are made of concrete (1:2:4) and is assumed very dry

initially. The thickness is taken as 12 mm. The vapor diffusivity, D_m, and vapor permeability, δ_v, in the materials are taken from literature (Annex24, 1996). The floor of the room is covered with vinyl tile and it is assumed no adsorption and desorption. The initial water vapor density in the room, ρ_{wv0}, is $0.0075\,kg/m^3$ (RH=75% at 11 °C) and moisture diffusivity in the room air is considered a constant as $2.63\times10^{-5}\,m^2/s$ (Wong and Wang, 1990; Keresteciogl u and Gu, 1990). The convective heat and mass transfer coefficient can be calculated by Equations 3-34 to 38. All input parameters are shown in Table 3-6. The simulation is carried out until the indoor humidity reaches a steady state.

Table 3-5 Values of temperature and convective heat transfer coefficients in the exterior walls, temperature in °C, heat transfer coefficients, h_T, $w/m^2\cdot k$
(from Wurtz et al., 1999b)

	East wall	West wall	North wall	South wall	Ceiling	Floor
Temperature (° C)	14.1	14.1	13.9	6.0	13.5	11.8
Heat transfer coefficient (w/m^2k)	4.1	4.1	4.1	4.1	5.7	1

Table 3-6 Values of the input parameters for case 1

Parameter	ρ_{wv0}	ρ_{m0}	D_m	D_a	δ_v	b
(unit)	kg/m^3	kg/m^3	m^2/s	m^2/s	m^2/s	m
Value	0.0075	0	2.89×10^{-10}	2.63×10^{-5}	6.42×10^{-7}	0.012

In this study, due to the same physical configurations (MINIBAT tests), a grid number of 6×3×6 is used, the temperature distribution and the airflow pattern within the room are the same as the prediction made by Huang (2003), and it was compared and validated with literatures (Haghighat *et al.*, 2001; Jiang, 1998; Inlard *et al.*, 1996), as shown in Figure 3-9 and Figure 3-10.

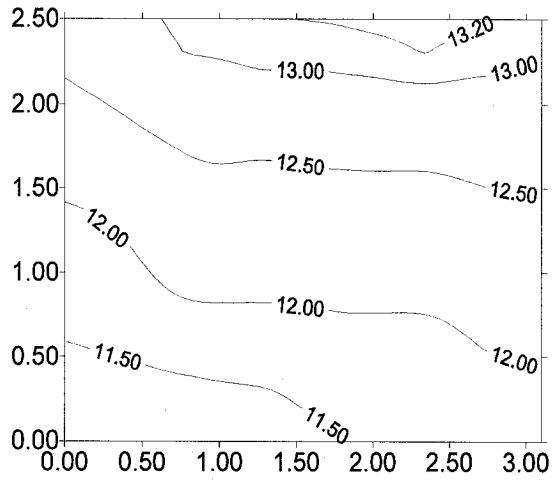

Proposed Model
(6×3×6 zones)

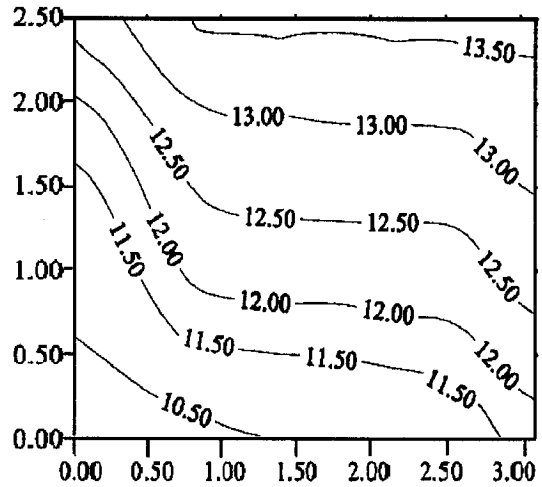

POMA (6×1×10 zones)
(Haghighat et al., 2001)

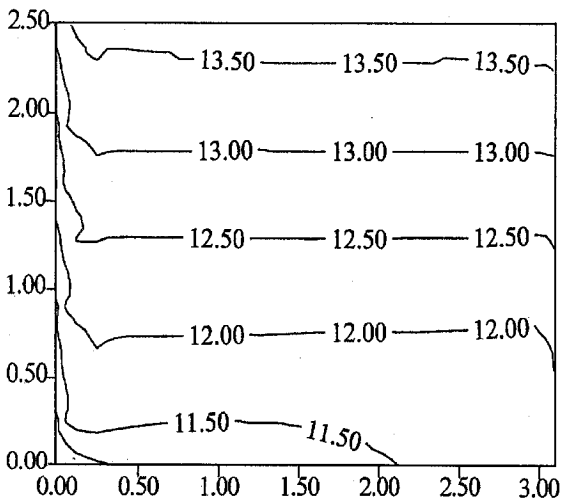

CFD Model (41×51×41 zones)
(Jiang, 1998)

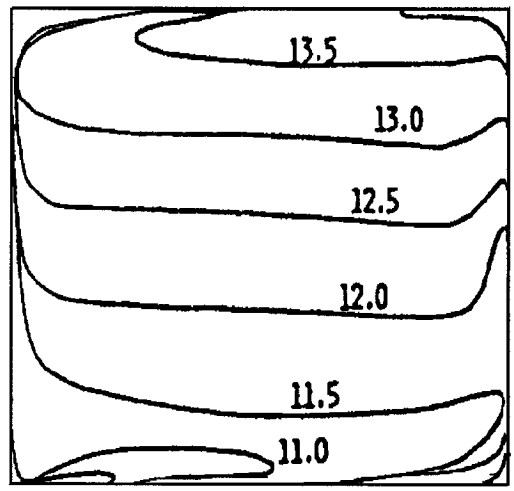

Experiment Results
(Inard, 1996)

Figure 3-9 Comparison and validation of temperature distributions for case 1

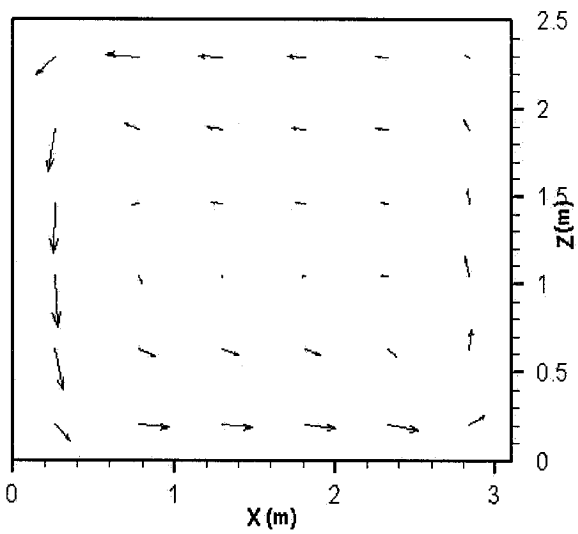

Proposed Model
(6×3×6 zones)

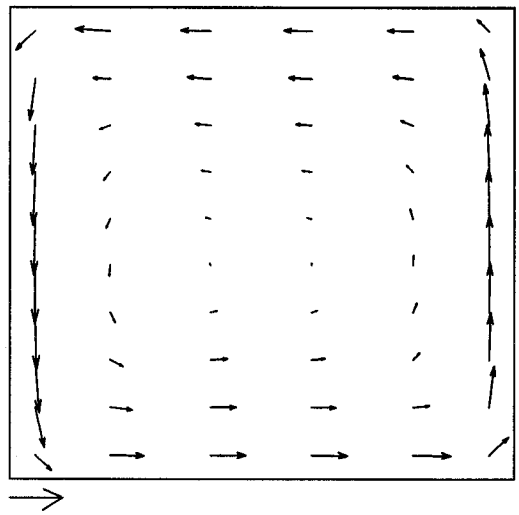

POMA (6×1×10 zones)
(Haghighat et al., 2001)

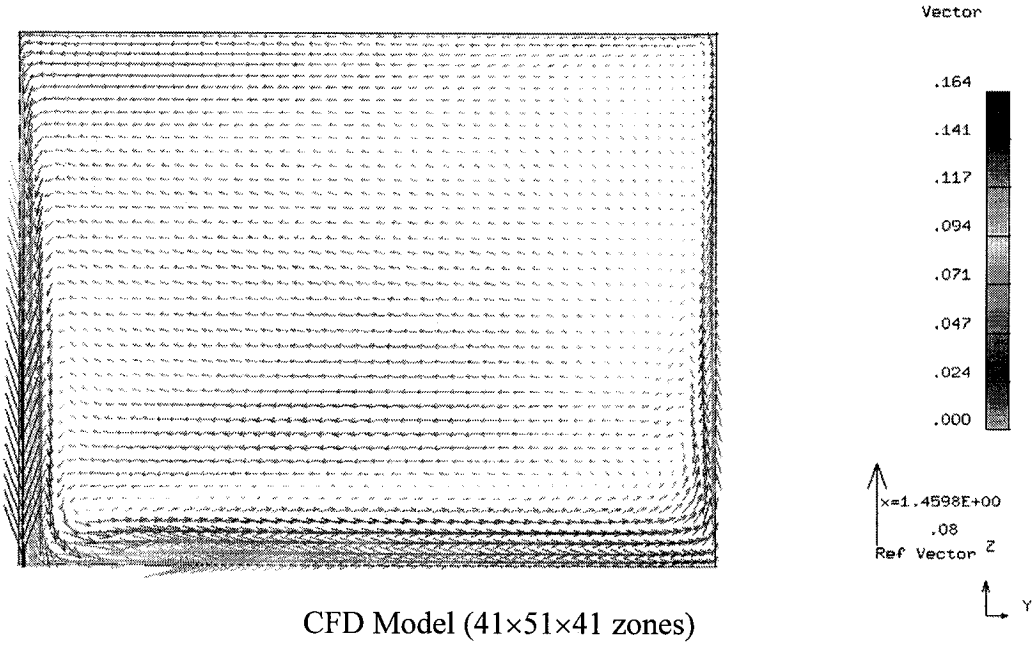

CFD Model (41×51×41 zones)
(Jiang, 1998)

Figure 3-10 Comparison of air flow patterns for case 1

Water vapor density distributions are graphically displayed in Figures 3-11, 3-12 and 3-13 for the middle section of the room after the dry walls are exposed to the air for 1 hour, 3 hours, and 12 hours. The figures show that water vapor density is not uniform in the room at the beginning and is affected by the airflow pattern, as shown for the time of 1 hour after exposure. Water vapor density is higher in the middle regions than the regions close to walls due to moisture adsorpted by wall materials. Gradually, water vapor density becomes uniform in the room, as shown for the time 12 hours after the exposure. This is because the room water vapor density eventually reaches the steady state condition.

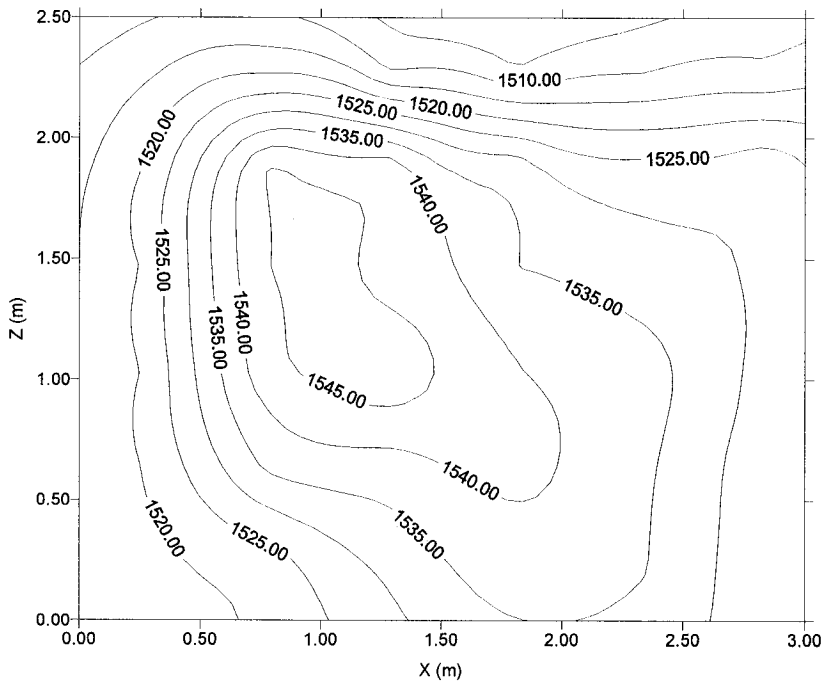

Figure 3-11 Water vapor density (mg / m^3) distribution after 1 hour for case 1

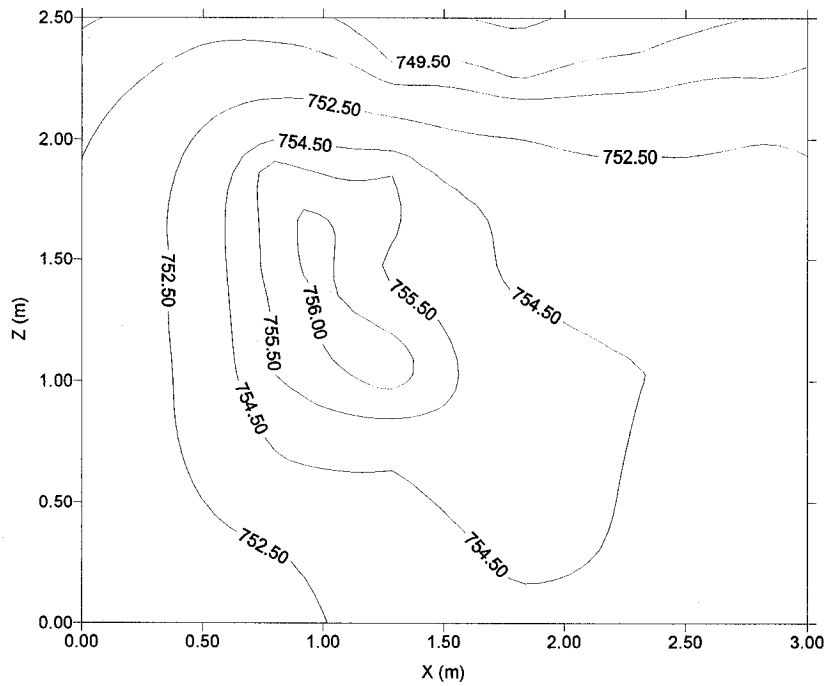

Figure 3-12 Water vapor density (mg / m^3) distribution after 3 hour for case 1

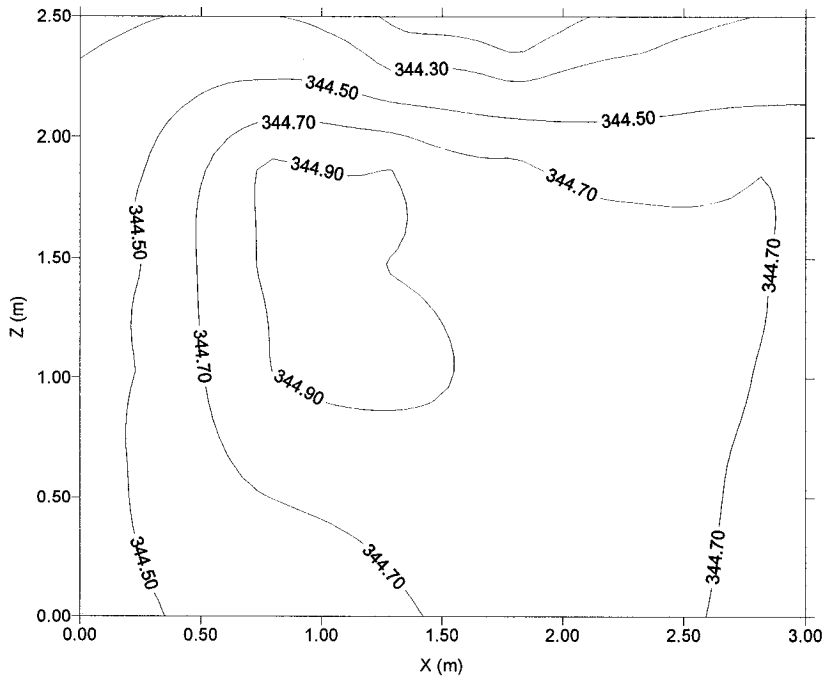

Figure 3-13 Water vapor density (mg / m^3) distribution after 12 hour for case 1

The average water vapor density in the room air decreases very fast initially. As time passing, it gradually reaches a steady state, as shown in Figure 3-14, since it is not mechanically ventilated. In this study, the wall materials' sorption rate is also predicted, as shown in Figure 3-15. The results take the east wall as example and show that the adsorption rate decreases initially and over time finally reaches a steady state. The minus sign indicates that the direction of the water vapor transport is from indoor materials to indoor air.

Moreover, Figure 3-16 shows the corresponding average water vapor density in the room with and without adsorption /desorption. It gives significantly different behavior. The water vapor density is almost constant when adsorption /desorption is not considered; otherwise it decreases significantly over time. This result implies that adsorption and desorption significantly influences the moisture distribution in a non-ventilated room.

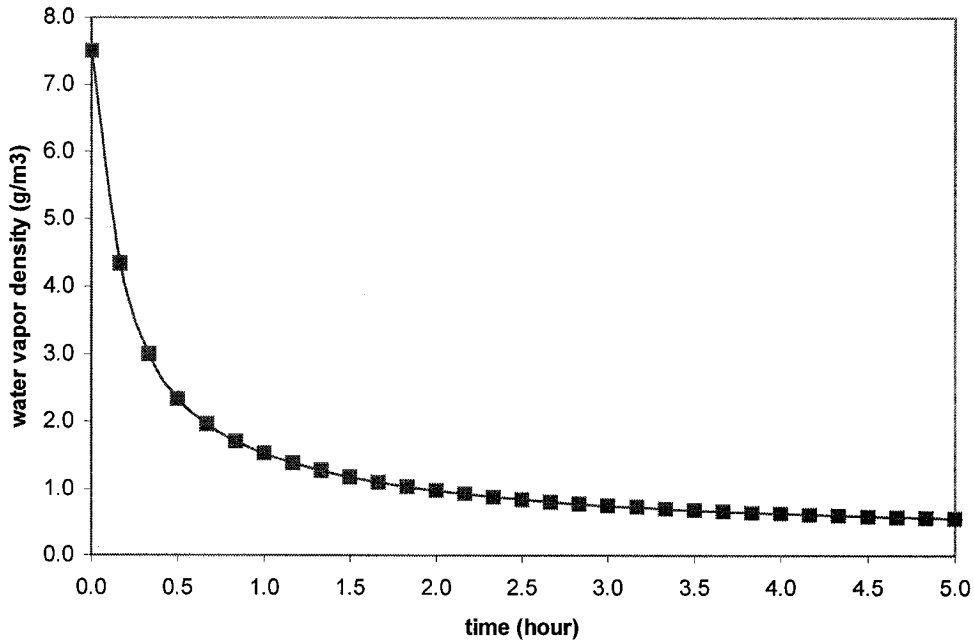

Figure 3-14 Average water vapor density in the room air for case 1

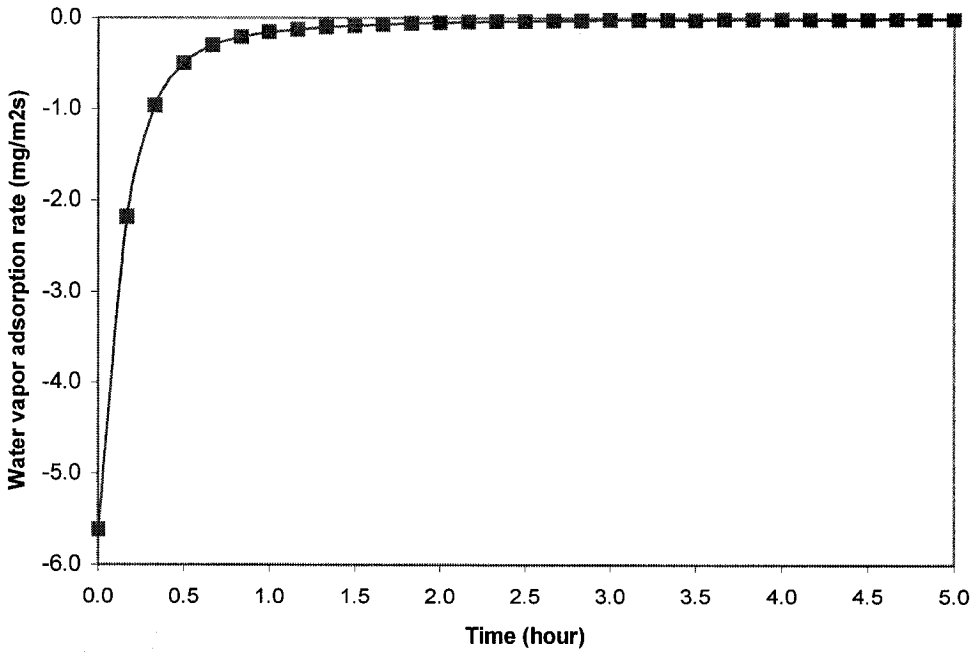

Figure 3-15 Average water vapor adsorption rate of east wall for case 1

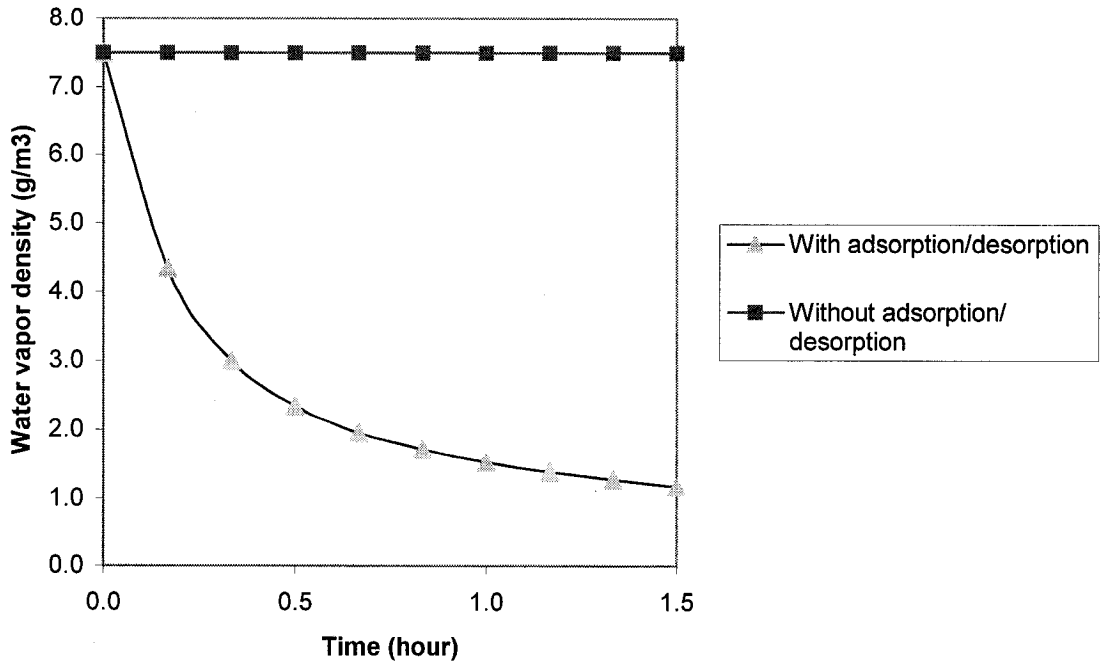

Figure 3-16 Comparison of average water vapor density in the room air with and without adsorption/ desorption for case 1

3.6.2 Case 2: Natural ventilation

Besides predicting water vapor distribution in the room air, the proposed model also could predict the effect of moisture adsorption/ desorption on interior surfaces of the wall.

Condensation, which transfers the water vapor from its harmless form to its problem-causing liquid form, is the first indication of the rising potential of moisture problems. For indoor conditions, wall moisture levels will quickly respond to any changes in the indoor air humidity due to moisture transport between the wall system and the indoor air. In addition, for condensation to occur at any point in the wall system, the local partial

pressure must exceed the saturation vapor pressure corresponding to the temperature at that point. Therefore, a sudden rise in indoor humidity or descend in temperature, even for a short period of time, may result in condensation within the wall.

In this case study, by predicting water vapor density and temperature distribution at the wall surface, it can be shown that proposed models can predict the occurrence of condensation, and the resulting damaged wall. The physical configuration and input parameters are followed.

The proposed model is applied to a naturally ventilated room. The presented room has an opening (air inlet) at the top of the west wall and one air outlet at the bottom of the opposite wall. The dimension of the room is $3.0 \times 3.0 \times 2.5 m^3$ and the air exchange rate is $0.0075\, kg/s$ (1ACH). The room condition is taken as non-isothermal. The concrete (1:2:4) is taken as the interested material and the thickness is 12 mm. The temperature at the west wall is 18 °C and the other walls and ceiling are 23 °C. The initial water vapor density in the room, ρ_{wv0}, is $0.018\, kg/m^3$ (RH=87.5% at 23 °C), and for inlet air, the water vapor density is equal to the water vapor density in the room air and temperature is 31 °C. The initial water vapor density of the envelope material, ρ_{m0}, is assumed as $0.01\, kg/m^3$ (RH=65.1% at 18 °C for the west wall and RH=48.6% at 23 °C for other walls). The floor is covered by vinyl tile and it is assumed no adsorption and desorption. The vapor diffusivity, D_m, and vapor permeability, δ_v, in the materials are taken from literature (Annex24, 1996). All input parameters are shown in Table 3-7.

Table 3-7 Values of the input parameters for case 2

Parameter	ρ_{wv0}	ρ_{m0}	D_m	D_a	δ_v	b
(unit)	kg/m^3	kg/m^3	m^2/s	m^2/s	m^2/s	m
Value	0.018	0.01	2.89×10^{-10}	2.63×10^{-5}	6.42×10^{-7}	0.012

First, the proposed model is used to predict the temperature distribution in the room air, as shown in Figure 3-17. Water vapor density distributions are graphically displayed in Figures 3-18 and 3-19 for the middle section of the room after the walls are exposed to the air for 1 hour and 12 hours.

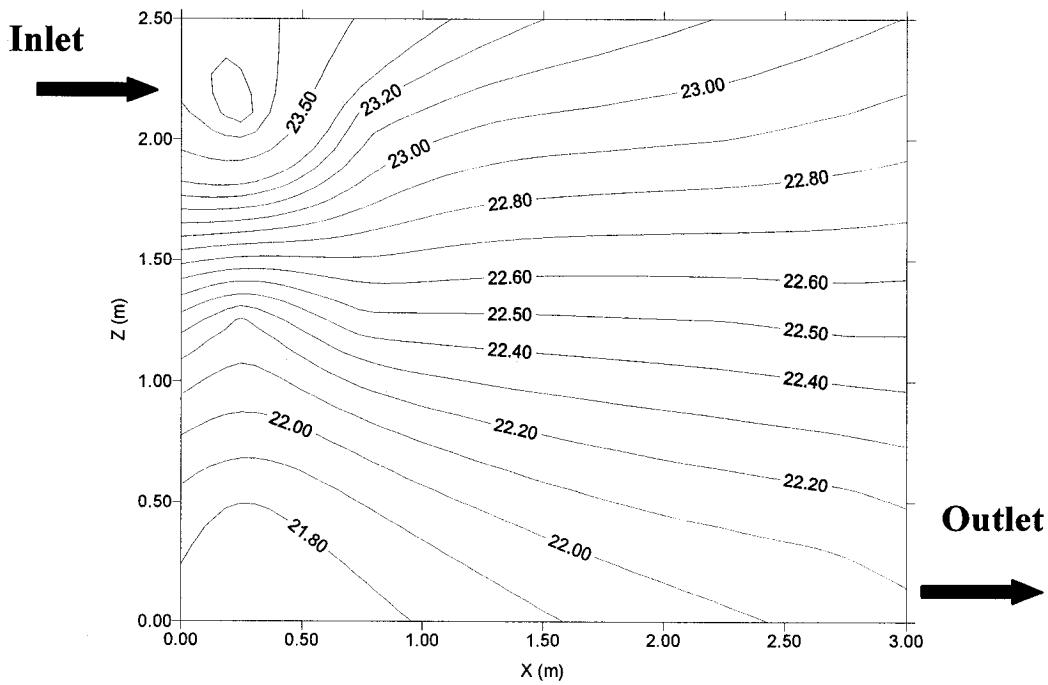

Figure 3-17 Temperature distribution (° C) in the middle section of the room for case 2

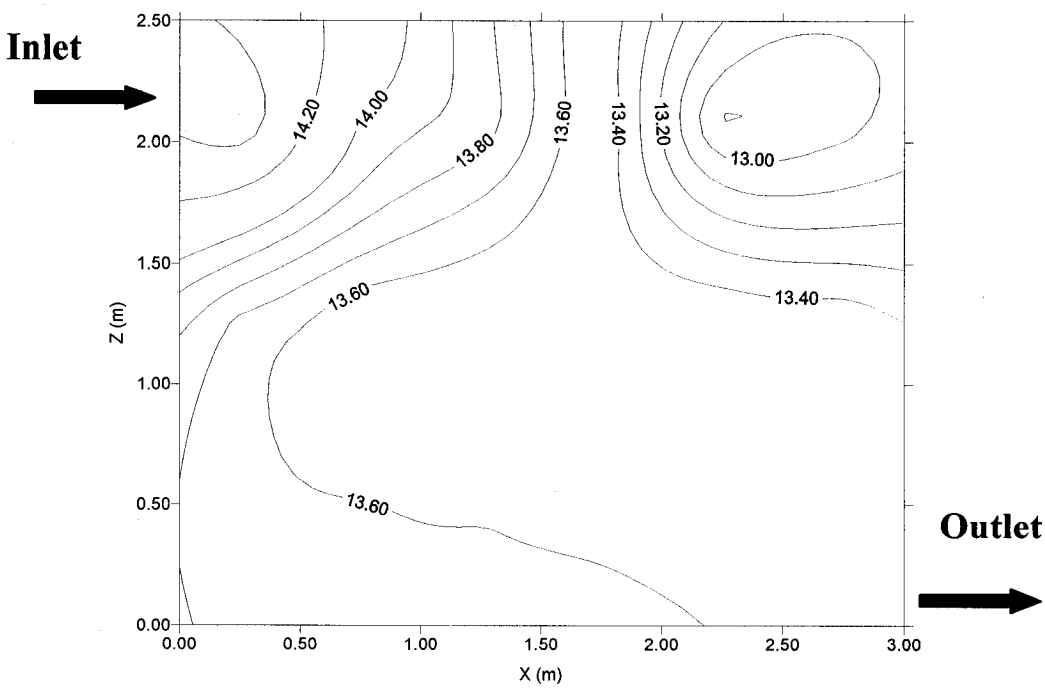

Figure 3-18 Water vapor density (g / m^3) distribution after 1 hour for case 2

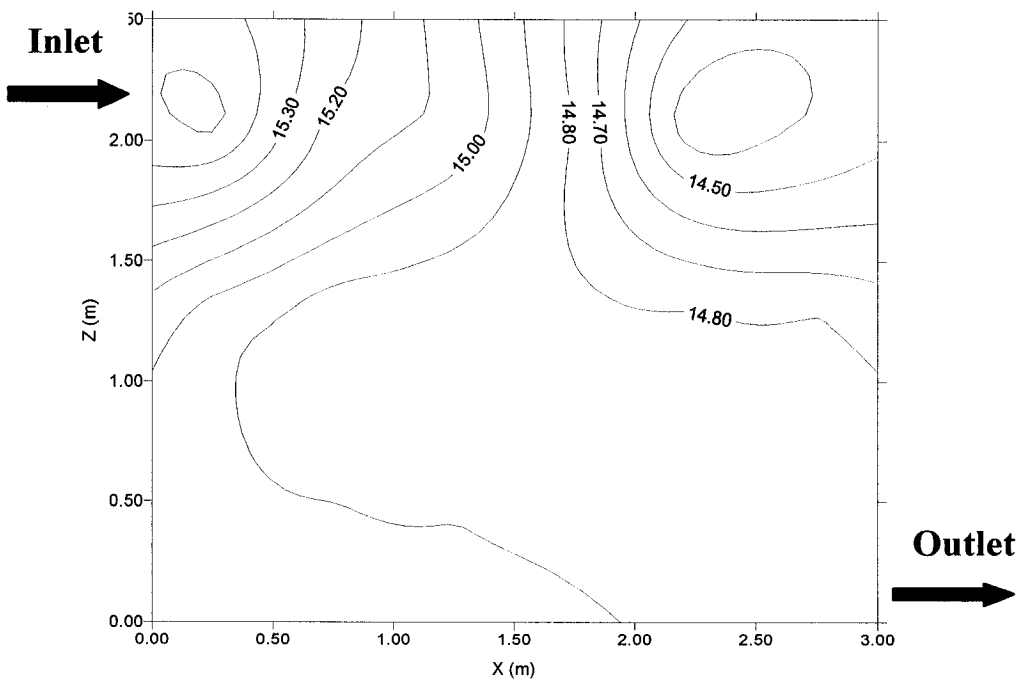

Figure 3-19 Water vapor density (g / m^3) distribution after 12 hours for case 2

The average water vapor density in the room for 40 hours is shown in Figure 3-20. At first, water vapor transfer very fast between indoor air and interior materials, thus the average water vapor density decreases as time progressed. There is a peak as shown in the figure. And then, with time increasing, water vapor density gradually increases due to less water vapor adsorption by the interior material surfaces and continuous air supply from the inlet. These results also are confirmed by water vapor adsorption rate curves, as shown in Figure 3-21. Water vapor adsorption rate of the wall decreases as time increased.

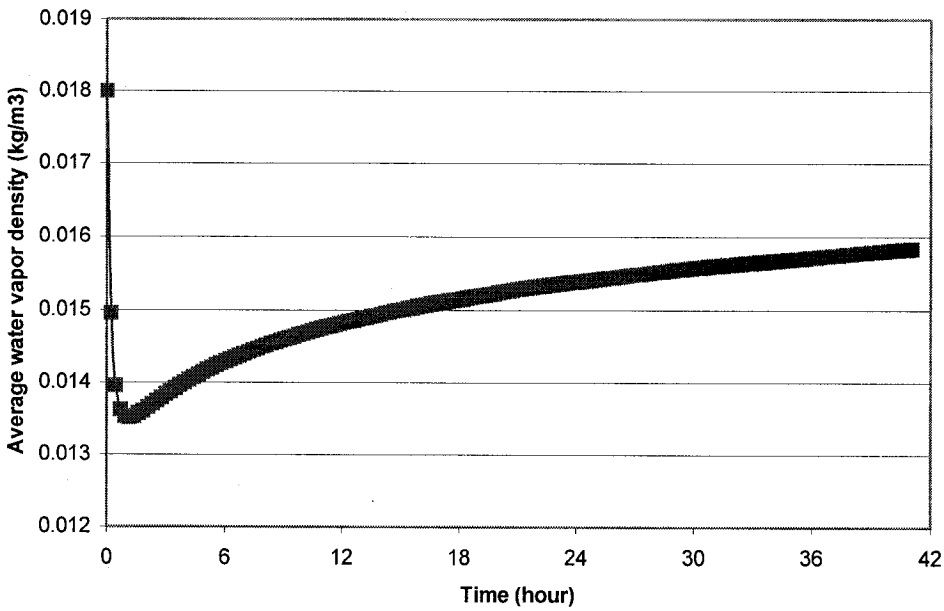

Figure 3-20 Average water vapor density in the room air for case 2

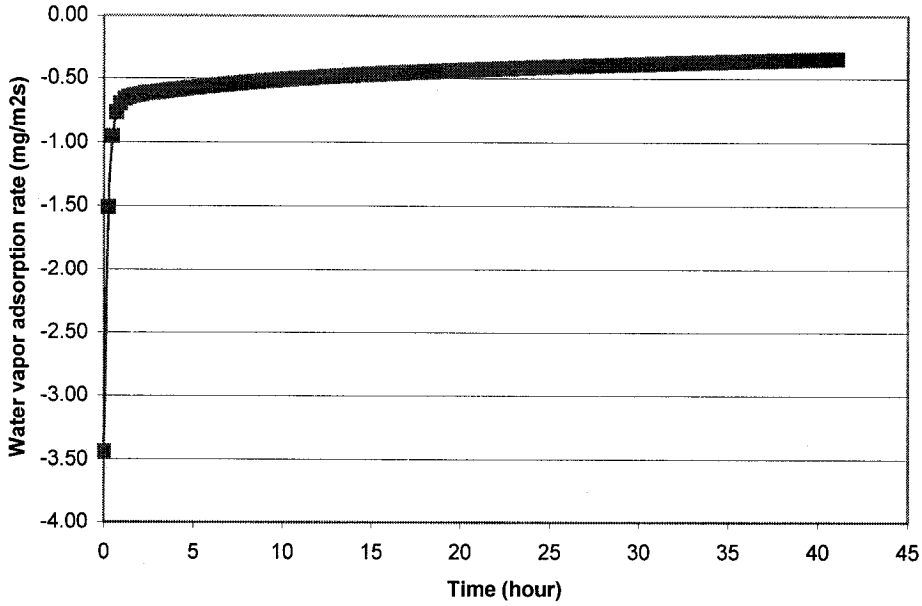

Figure 3-21 Average water vapor adsorption rate of east wall for case 2

In this case, since the west wall has a relatively lower temperature and high humidity level by adsorption from indoor air which has a high relative humidity, the condensation occurs at the surface of west wall. Figure 3-22 shows the comparison of water vapor density in the middle section of the west wall (Z=0.42m) for 45 hours with the saturated water vapor density. When water vapor density is higher than saturated water vapor density at 18 °C ($15.36\, g/m^3$), water vapor will condense. Figure 3-22 shows that water vapor density at the surface of the west wall reaches a saturated value at the 40^{th} hour; this means condensation will occur at the surface of the cold wall. Therefore, this case demonstrates further that the adsorption and desorption influence not only the indoor air humidity distribution, but the envelope system as well.

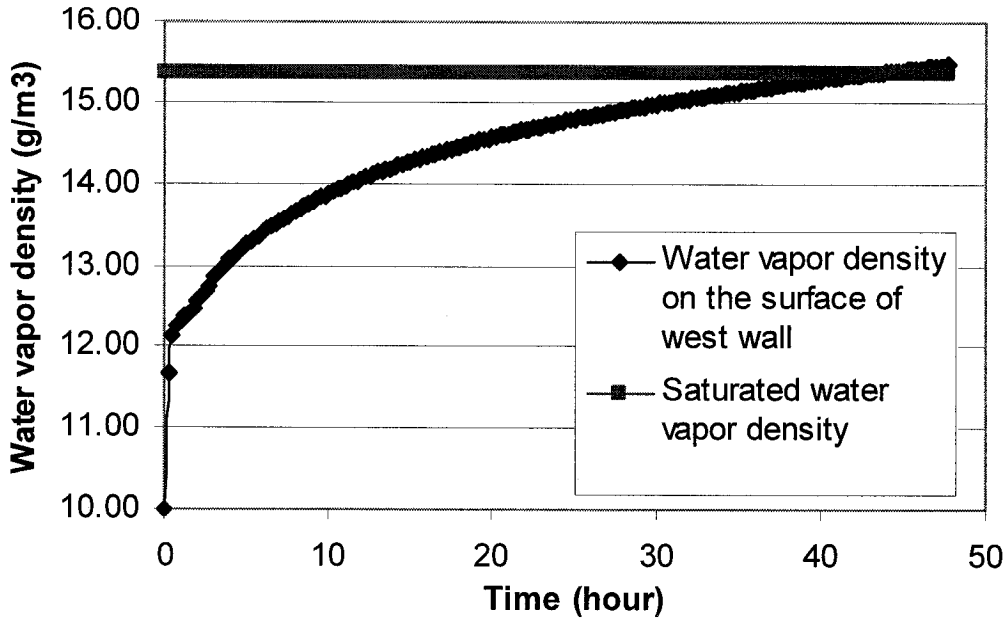

Figure 3-22 Comparison of water vapor density at the surface of west wall with the saturated vapor density for case 2

3.6.3 Case 3: Forced ventilation with 2D linear air jet

Unlike naturally ventilated room with opening (case 2), this case studies a room with mechanical system with a two-dimensional linear air jet on the west wall and an outlet at the bottom of the east wall. The physical configuration adopted here is the same as Huang's model (2003), as shown in Figure 3-23. The dimensions of the room are $3.0\times3.0\times2.7m^3$ and at an isothermal condition with temperature at 23 °C. The inlet airflow rate is 0.08 kg/s, and water vapor density is same as initial indoor water vapor density.

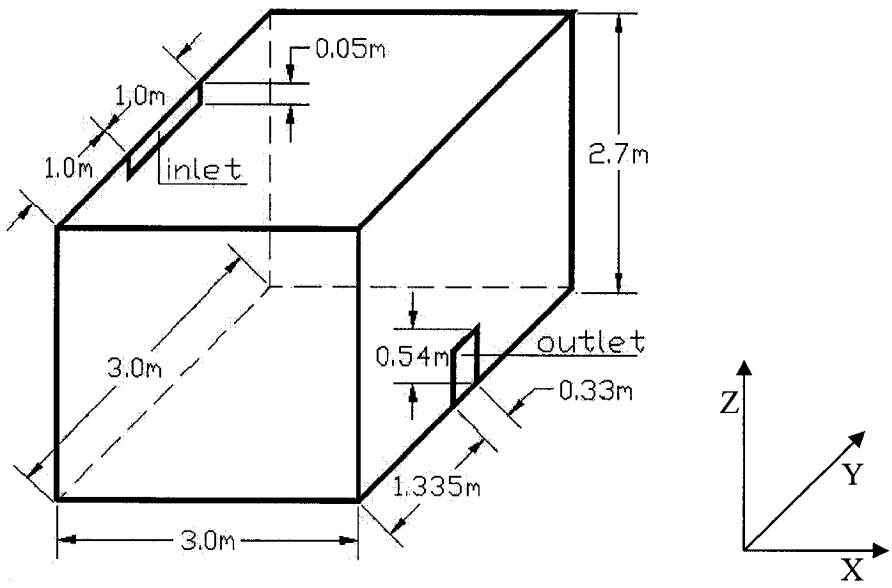

Figure 3-23 Geometry of the room with a linear jet (from Huang, 2003)

Since the physical configuration is similar to the indoor conditions are used, the airflow pattern within the room will be similar to Huang's model (Huang. 2003), and it is validated by comparison with that of the commercial CFD software FLOVENT (Jiang, 2002).

The airflow patterns in the middle section of the room, simulated by the Integrated Zonal Model and the CFD model, are graphically shown in Figures 3-24 and 3-25. Globally, a similar airflow pattern is achieved in both models. A strong air stream along the ceiling and a circulation around the middle of the room are detected in both models.

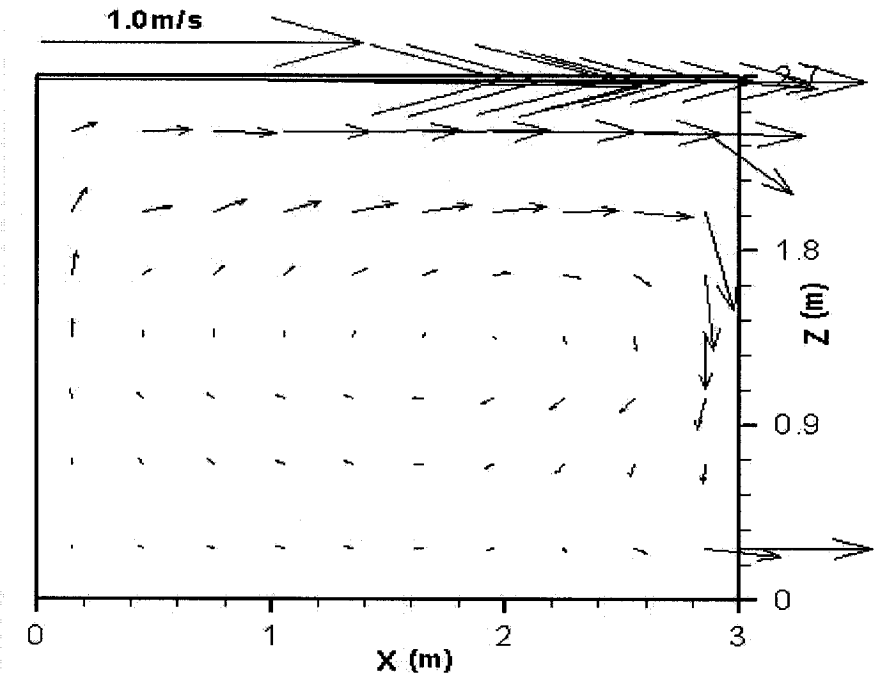

Figure 3-24 Air flow pattern predicted by the Integrated Zonal Model for case 3

(grids: 10×3×8) (Huang, 2003)

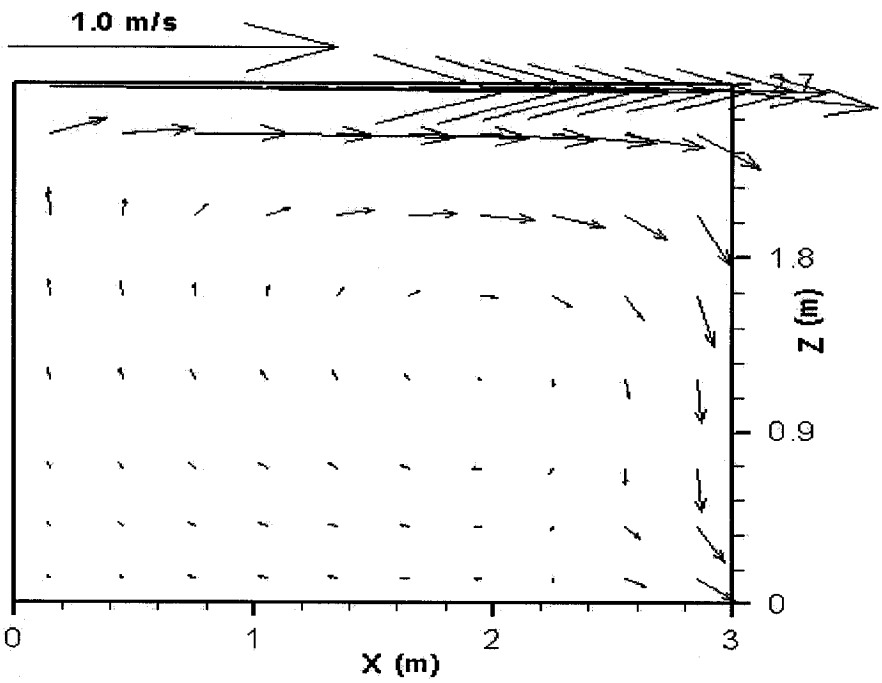

Figure 3-25 Air flow pattern predicted by FLOVENT for case 3

(grids: 10×9×8) (Jiang, 2002)

For the simulation of indoor air humidity, four walls (east, west, south and north wall) are assumed to use gypsum board as the material of interest. The ceiling is decorated with plywood. The floor of the room is covered with vinyl tile and it is assumed there to be no moisture adsorption or desorption. The initial water vapor density in the room, ρ_{wv0}, is $0.01\,kg/m^3$ (RH=50% at 23 °C). For the building envelope, the initial water vapor density is assumed as $0.002\ kg/m^3$ (RH=10% at 23°C). The vapor diffusivity, D_m, and vapor permeability, δ_v, in the materials are taken from literature (Annex24, 1996). All input parameters are shown in Table 3-8.

Table 3-8 Values of the input parameters for case 3

Parameter	ρ_{wv0}	ρ_{m0}	D_m	D_a	δ_v	b
(unit)	kg/m^3	kg/m^3	m^2/s	m^2/s	m^2/s	m
Plywood	0.01	0.002	3.2×10^{-13}	2.63×10^{-5}	3.55×10^{-8}	0.0065
Gypsum Board	0.01	0.002	1.8×10^{-8}	2.63×10^{-5}	3.72×10^{-6}	0.1

Water vapor densities are distributed in the middle section of the room (Y=1.5m) for time of 0.5 hour, 2 hours and 12 hours are graphically displayed in Figures 3-26, 3-27 and 3-28. Initially, water vapor density is not uniform due to water vapor adsorption by the interior surface of the wall. Gradually, water vapor density reaches the steady state condition due to the mechanical ventilation system.

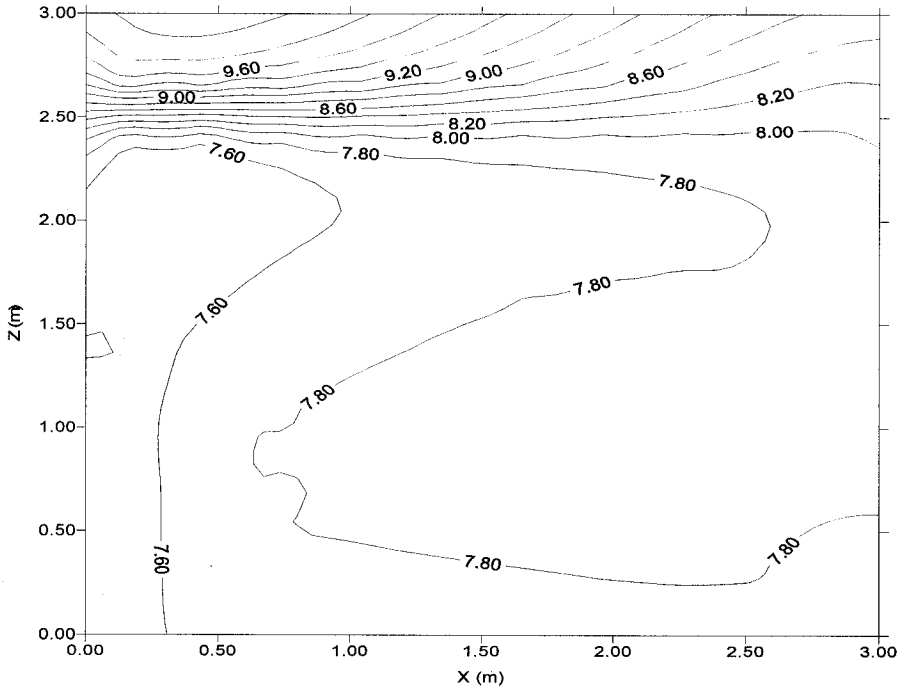

Figure 3-26 Water vapor density (g / m^3) distribution in the room air for case 3 (0.5 hour)

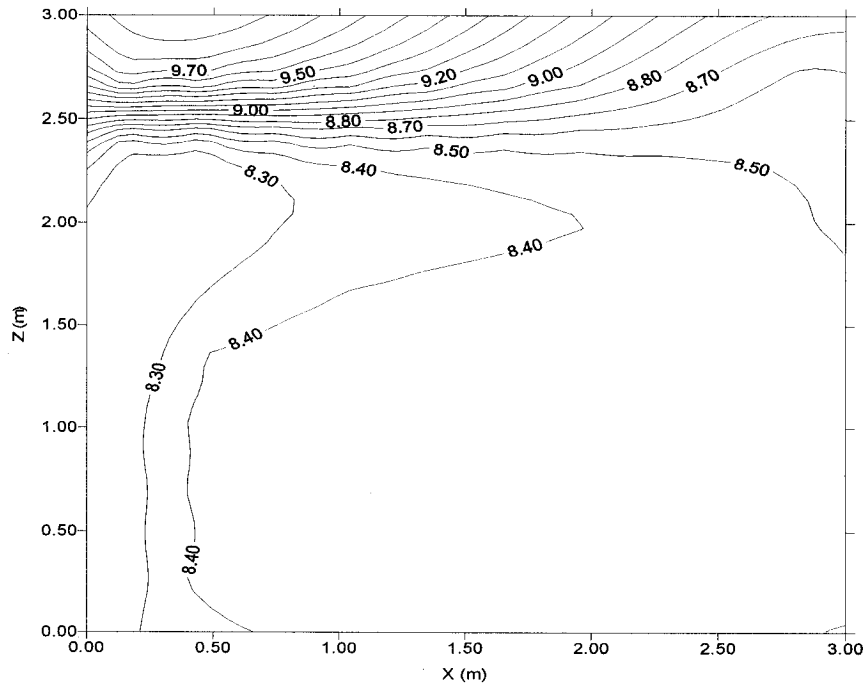

Figure 3-27 Water vapor density (g / m^3) distribution in the room air for case 3 (2 hours)

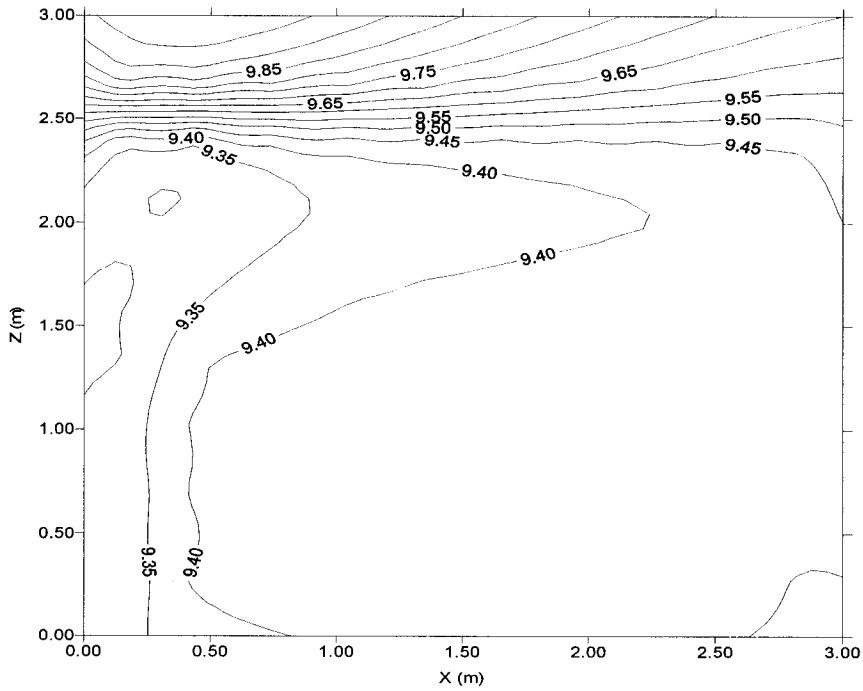

Figure 3-28 Water vapor density (g / m^3) distribution in the room air for case 3 (12 hours)

In addition, the average water vapor density distribution in the room air for 10 hours and 100 hours, as shown in Figures 3-29 and 3-30, show that it takes almost 20 hours before the average water vapor density reach steady state condition. Meanwhile, the water vapor adsorption rate of building materials for times 10 and 100 hours, as shown in Figures 3-31 and 3-32, indicates that the water vapor adsorption rate also decreases with time gradually and reaches the steady state condition rapidly. These results demonstrate that the mechanical ventilation system influences moisture adsorption and desorption of the interior surface of the wall and indoor humidity distribution timely.

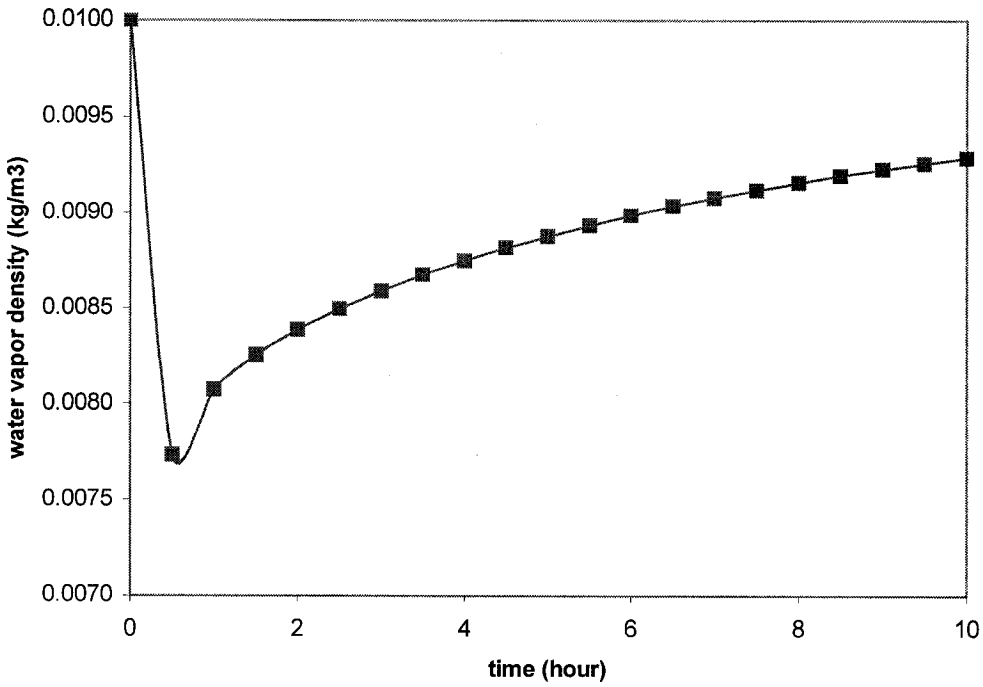

Figure 3-29 Average water vapor density in the room air for case 3 (10 hours)

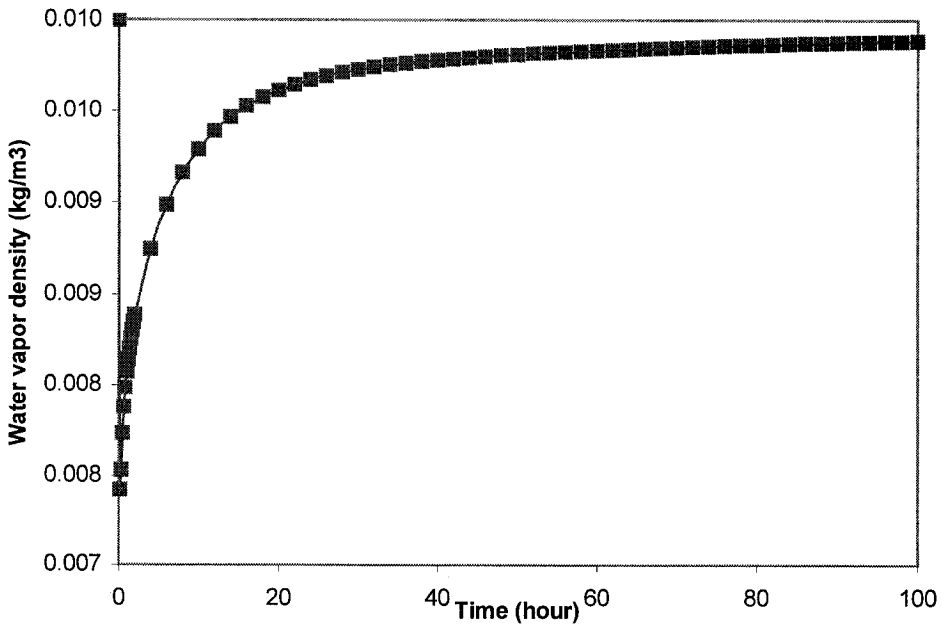

Figure 3-30 Average water vapor density in the room air for case 3 (100 hours)

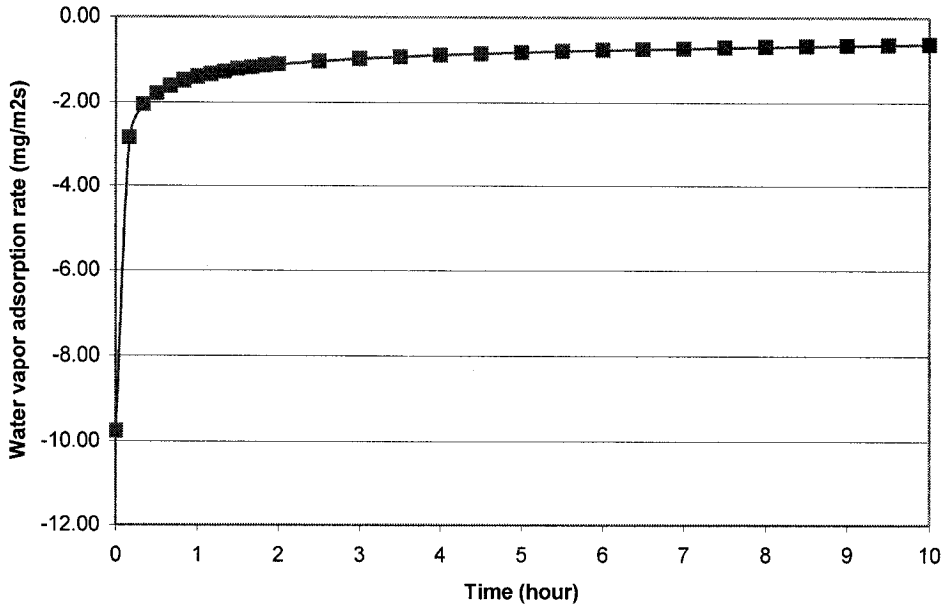

Figure 3-31 Average water vapor adsorption rate by west wall for case 3 (10 hours)

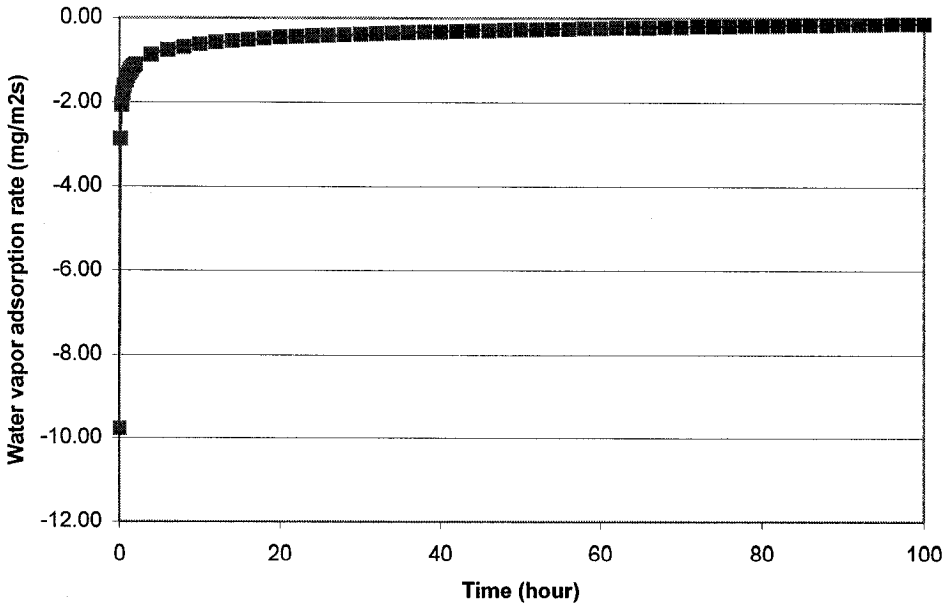

Figure 3-32 Average water vapor density adsorption rate by west wall for case 3 (100 hours)

The average water vapor sorption rates from the west, east, south, and north walls and from the ceiling for the first 2 hours are shown in Figure 3-33. The minus sign represents water vapor transport from indoor to materials. First, compared with the walls, the ceiling has the higher sorption rate, which is mainly because the plywood is much thinner than the gypsum board. Second, Figure 3-33 also shows that for four walls, the region close to the east wall has the highest water vapor adsorption rate initially, except for the ceiling. It is due to the higher air velocity along the east wall as compared the velocity along the other walls. Velocity has a significant impact on the sorption rate for the first 20-30 minutes. The reason is that at the beginning the initial water vapor density at the gypsum board surface is relatively low; therefore the adsorption rate increases as the velocity increases. As time passing, the velocity effect diminishes, so adsorption rates becomes independent of the air velocity, as shown in Figure 3-33. The adsorption rates from the four walls are very close to each other. This is because the internal diffusion dominates the sorption process. Finally, the south wall and the north wall have the same sorption rate due to the symmetry of the airflow.

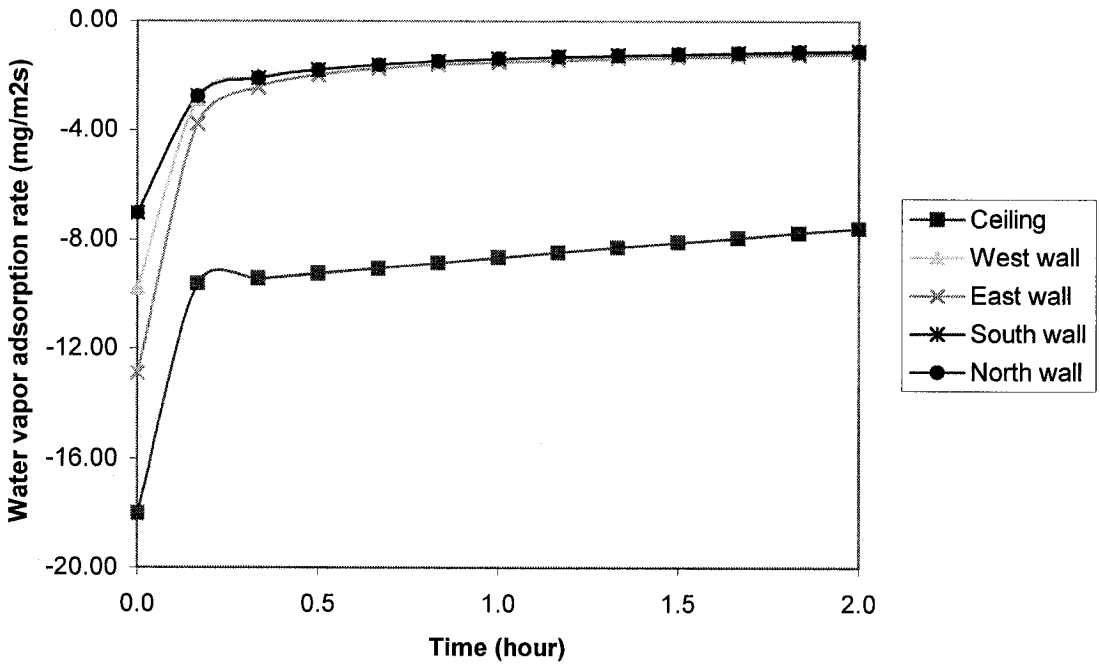

Figure 3-33 Average water vapor adsorption rate in the room air for case 3

3.7 Summary

An Integrated Zonal Model has been developed to predict the three-dimensional air flow profile, temperature distribution, and water vapor density distribution in a ventilated room and in an envelope. This model is integrated into a zonal model with a moisture transfer in the material model and taking into account material moisture adsorption and desorption effect.

This Integrated Zonal Model is firstly applied to a non-ventilated room. The room is in a non-isothermal condition with very dry wall material. By comparison, water vapor density vs. time in the room with and without adsorption and desorption finds that

adsorption and desorption has influence on indoor humidity distribution. Moreover, the simulation results also indicate that the water vapor density is not uniform in the space initially but reaches the steady state condition gradually, in which the water vapor density becomes uniform.

The Integrated Zonal Model is also applied to a naturally ventilated room to predict water vapor distribution within the room and the effect of moisture adsorption and desorption on an envelope system. The room is in a non-isothermal condition and naturally ventilated. It has been found that, due to moisture adsorption and desorption, water vapor density in the materials can increase vs. time and probably reach a saturated condition. This would allow condensation to occur and possibly damage walls. For avoiding condensation, it is very necessary to accurately simulate both an indoor humidity distribution.

Finally, for more practical purposes, the proposed model is used to simulate the airflow pattern and the moisture distribution within a room and envelope system with a two-dimensional liner jet. The room is in an isothermal condition with four walls and a ceiling acting as the moisture sorption materials. The airflow pattern predicted by the Integrated Zonal Model (Huang, 2003) is compared with that of FLOVENT. Similar airflow patterns are detected in both models. Compared with natural ventilation case (case 2), the simulation results show that in a mechanically ventilated room moisture adsorption and desorption has influence on indoor air humidity distribution initially and soon reaches the steady state. Furthermore, it is found that air velocity affects moisture adsorption or

desorption only in short term when water vapor density at materials' surfaces are relatively high or low.

Overall, the Integrated Zonal Model, with a quite coarse mesh, could provide sufficiently reliable results and some global information regarding the airflow pattern, temperature, and water vapor density distributions within a room and envelope system.

Chapter 4

CONCLUSION AND RECOMMEDATION

4.1 Conclusions

A moisture transfer model was developed. This model then was integrated with an existing zonal model (Huang, 2003) to predict moisture concentration and distribution within the material and room air. The prediction of model was validated based on a critical literature review. This integrated zonal model is based on the conservation of air mass, energy, and water vapor mass, and it has been utilized to predict the three-dimensional air velocity profile, temperature distribution, and water vapor density distribution in the room and building materials under different conditions.

The case studies are carried out for investigating transient air humidity behavior in a non-ventilated or mechanically ventilated room at different physical and functional characteristics to simulate airflow pattern, temperature, and indoor humidity distributions. Based on the transient evaluation of indoor air humidity, the following findings have been drawn:

- Moisture adsorption and desorption by the interior surface of the wall can have significant impact on indoor air humidity distribution depending on the moisture and physical characteristics of the interior materials as well as the mechanical system.
- The prediction of indoor air humidity distribution within a space can significantly help assessing the potential risk of surface condensation.

- The knowledge of indoor air humidity distribution could also help evaluating the humidification and dehumidification requirements of a space over a particular period of time; hence, the requirements in energy consumption will be modified.

In summary, the results show that this Integrated Zonal Model could provide sufficiently reliable information about indoor humidity distribution within a room and building materials. It could be used to examine the impact of an air distribution system on the indoor humidity distribution within a room, and to analyze building material adsorption and desorption behaviors in order to accurately control mechanical systems and decrease energy consumption. Furthermore, through the case study, it is found that the Integrated Zonal Model is a feasible approach for building material moisture distribution analysis for the viewpoint of engineering.

4.2 Recommendations

As an enhancement and a continuation of investigating moisture adsorption and desorption behavior and its effect on indoor air quality (IAQ) and energy analysis, the following recommendations and for the future studies and the limitations for the present work can be written as:

- The major problem is the lack of material property data. Extensive literature surveys indicate that moisture data is primarily limited to food products and is unknown for many common building materials. It should be pointed out that many of the

parameters given in the literature are not directly applicable to surface adsorption and desorption. Therefore, extensive experimental research is needed to establish the described moisture transport parameters for a wide range of common building materials. Besides moisture properties, evaluation of the convective mass transfer coefficient is also very important since moisture transport from the surfaces of a solid is dominated by convective fluxes.

- The proposed model needs experimental data for further validation. Since there is a lack of relevant experimental data, the proposed model only did some general validations on moisture conditions on the surface of the materials and desorption rate for particular materials. A deep validation and investigation of the effects of moisture adsorption and desorption on indoor air humidity behavior and moisture condition in various building materials are needed.

- The indoor air humidity prediction model developed in this study could be further integrated with other energy analysis and indoor air quality (IAQ) models.

- Future humidity distribution modeling research should concentrate on integration with more models, taking into account more appropriately the air heat transfer, energy analysis, and balance by means of evaporation or condensation of water vapor in indoor air, as well as condensation phenomena on enclosure surfaces. On this subject, the results of natural ventilation case (case 2) have revealed a good potential to ameliorate the combined modeling of heat, moisture and air transport.

REFERENCE

Adamson, A. W., (1990), Physical chemistry of surface, *Wiley-interscience Publication*, New York

Allard, F. and Inard, C., (1992), Natural and mixed convection in rooms: prediction of thermal stratification and heat transfer by zonal models, *ISRACV, 1992, pp.* 335-342

Allard, F., (1987), Contribution a l'étude des transferts de chaleur dans les cavites thermiquement entrainees: application aux cellules d'habition (Contribution to the study of heat transfer in thermally entrained cavities: application to rooms). Ph.D thesis, INSA de Lyon, France

Andesson, A.C., (1985), Verification of calculation methods for moisture transport in porous building materials, *Swedish council for building research, Document D6*

L'Anson, S.J., Hoff, W.D., (1986), Water movement in porous building materials- VIII Effect of evaporative drying on height of capillary rise equilibrium in walls, *Building and Environment* 21(3/4), *pp.*195-200

ASHRAE Fundamentals, (2001), Thermal and moisture control in insulated assemblies – fundamentals. *ASHRAE Fundamentals Handbook*

Annex24, (1996), Annex 24 Report on material properties, Building Performance Laboratory, Institute for Research in Construction, National Research Council, Canada

Axley, J.W., (1991), Adsorption modeling for building contaminat dispersal analysis, *Indoor Air, Vol. 1, pp.* 147-171

Axley, J.W., (2001), Surface-drag flow relations for zonal modeling, *Building and Environment* 36, *pp.* 843-850

Barringer, C.G., McGugan, C.A., (1989), Development of a dynamic Model for simulating indoor air temperature and humidity. *ASHRAE Transactions, Vol.95, pp.*449-460

Bear, J. and Bachmat, Y., (1990), Introduction to modeling of transport phenomena in porous media, *Kluwer Academic Publisher, Dordrecht, the Netherlands*

Blondeau, P., Allard, F., and Tiffonnet, A.L., (2000), Étude du role des parois dans la gestion de la qualite de l'air interieur des batiments non-industriels, *Convention n0A97-19 entre le PUCA et l' Universite de la Rocjell*

Bomberg, M. (2003), Modern Building Materials, Class notes and course package,

Concordia University, Montreal, Quebec, Canada

Burch, D.M., Thomas, W.C., Mathena, L.R., Licitra, B.A., and Ward, D. B., (1995a), Transient heat and moisture transfer in multi-layer, non-isothermal walls – Comparison of predicted and measured results. *Proceedings of Thermal Performance of the Exterior Envelopes of Buildings IV, pp.* 513-531

Burch, D.M., Zarr, R.R., and Fanney, A.H., (1995b), Experimental validation of a moisture and heat transfer model in the hygroscopic regime. *Proceedings of Thermal Performance of the Exterior Envelopes of Buildings VI, pp.* 273-281

Cunningham, M.J., (1990a), Modeling of moisture transfer in structures – I, A description of a finite-difference Nodal model, *Building and Environment 25(1), pp.* 55-61

Cunningham, M.J., (1990b), Modeling of moisture transfer in structures – II, A comparison of a numerical model, an analytical model, and some experimental results, *Building and Environment 25(2), pp.* 85-94

Cunningham, M.J., (1992), Effective penetration depth and effective resistance in moisture transfer, *Building and Environment 27(2), pp.* 379-386

El Diasty, R., Fazio, P., and Budaiwi, I., (1993), Dynamic Modeling of Moisture Absorption and Desorption in Buildings. *Building and Environment Vol. 28, No.1, pp.* 21-32

Fairey, P.W., Keresteciogiu, A.A., (1985), Dynamic modeling of combined thermal and moisture transport in buildings: effects on cooling loads and space conditions. *ASHRAE Transactions, Vol. 91(2), pp.*461-472

Grunewald, J. and Houvenaghel, G., (2000), Documentation of the numerical simulation program DIM 3.1, Technical University of Dresden, Germany

Haghighat, F. and Megri, A.C., (1996), A Comprehensive validation of two aiarflow models—COMIS and CONTAM, *Indoor Air, March 1996, pp.* 278-288

Haghighat, F., Lin Y. and Megri, A.C., (2001), Development and validation of a zonal model-POMA, *Building and Environment* 36(1), *pp.*1039-1047

Hall, C., (1977), Water movement in porous building materials-I Unsatureted flow theory and its applications, *Building and Environment* 12, *pp.*117-125

Hall, C., Hoff, W.D., Nixon, N.R., (1984), Water movement in porous building materials-VI Evaporation and drying in brick and block materials, *Building and Environment* 19(1), *pp.*13-20

Hall, C., Kam-Ming Tse, T., (1986), Water movement in porous building materials- VII The Sorptivity of mortars, *Building and Environment* 21(2), *pp.*113-118

Hansen, K.K., Bertelsen, N.H., (1989), Results of a water vapor transmission round-robin test using cup methods, Water Vapor Transmission Through Building Materials and Systems: Mechanisms and Measurements, ASTM STP 1039, Trechesel, H.; Bomberg, M., Eds., *American Society for Testing and Materials, pp.* 91-99

Hens, H., (1996), Heat, air and moisture transport, final report: volume 1, Task 1: Modeling. *IEA Annex 24,* Laboratorium Bouwfysica, K.U.-Leuven, Belgium

Huang, Y., (2003), An engineering approximation of material characteristics for input to HAM model simulations, M.A.Sc thesis, Concordia University

Huang, H.Y. and Haghighat, F., (2002), Modeling of volatile organic compounds emission from dry building materials, *Building and Environment* 37, *pp.*1127-1138

Huang, H.Y., (2003), Modeling of volatile organic compounds emission and sink of building materials, Ph.D thesis, Concordia University

Hutcheon, N.B., and Handegord, G.O.P., (1989), Building Science for a Cold climate, second edition, NRCC, ISBN-09694266-0-2

Inard. C., Bouia. H., and Dalicieux. P., (1996), Prediction of air temperature distribution in building with a zonal model. *Energy and Buildings Vol. 24(2), pp.*125-132

Inard. C., (1988), Contribution a l'Étude du couplage thermique entre un emetteur de chauffage et un local, Ph.D thesis, INSA de Lyon, France

Isetti, C., Laurenti, L., and Ponticiello, A., (1988), Predicting vapor content of the indoor air and latent loads for air-conditioned environments: effect of moisture storage capability of the walls, *Energy and Buildings Vol. 12, pp.*141-148

Karagiozis, A., (2001), Advanced hygrothermal models and design models, *Proceedings of eSim 2001,* June 13-14, Ottawa, Canada

Karagiozis, A., Salonvaara, M., (1995), Influence of material properties on the hygrothermal performance of a high-raise residential wall, *ASHRAE Transactions, Symposia, CH-95-3-5, pp.* 647-655

Karger, J. and Ruthven, D.M., (1992), Diffusion in Zeolites and Other Microporous Solids, John Wiley & Sons, Inc.

Kast and Klan, (1982), Auslegung und prufung von fubbodenheizungen (Interpretation and test of floor heating), VDI-Berichte 464, pp. 39-49

Kelly, K.M., (1982), Indoor moisture effects on structure, comfort, energy, consumption and health. Thermal performance of the exterior envelope of buildings II, *Proceedings of the ASHRAE/DOE Conference, pp.* 1007-1032 Les Vegas, Nevada.

Keresteciogiu, A.A., (1989), Detailed simulation of combined heat and moisture transfer in building components. *Proceedings of Thermal Performance of the Exterior Envelopes of Buildings IV, pp.* 477-485

Keresteciogiu, A.A., and Gu, L., (1990), Theoretical and computational investigation of simultaneous heat and moisture transfer in buildings: "evaporation and condensation" theory, *ASHRAE Transactions, Vol. 96(2), pp.* 455-464

Keresteciogiu, A.A., Swami, M., and Kamel, A., (1990), Theoretical and computational investigation of simultaneous heat and moisture transfer in buildings: "effective penetration depth" theory. *ASHRAE Transactions. Vol. 96(1), pp.* 447-454

Kuenzel, H.M., Kiessl, K., (1997), Calculation of heat and moisture transfer in exposed building components. *International Journal Heat and Mass Transfer, Vol. 40, No. 1, pp.*159-167

Kumaran, M.K., (1989), Vapor transport characteristics of mineral fiber insulation from heat flow meter measurement, Water Vapor Transmission Through Building Materials and Systems: Mechanisms and Measurements, ASTM STP 1039, Trechesel, H.; Bomberg, M., Eds., *American Society for Testing and Materials, pp.* 19-27

Kumaran, M.K., (1992), Heat and moisture transfer trough building materials and components: can we calculate and predict? *Proceedings of the 6th conference on Building Science and Technology, pp.* 103-144, Waterloo, Canada

Kumaran, M.K., (1996), IEA Annex24: Heat, air, and moisture transport, Final report 3, task 3: material properties, Laboratorium Bouwfysica, K.U.-Leuven, Belgium

Kusuada, T., (1983), Indoor humidity calculations, *ASHRAE Transactions. Vol. 89(2), pp.*728-740

Kusuada, T., Miki, M., (1985), Measurement of moisture content for building interior surfaces, Moisture and Humidity 1985: Measurement and Control in Science and Industry, *Proceedings of the 1985 International Symposium, pp.* 297-311

Layman, W.J., (1982), Handbook of Chemical Property Estimation Methods, New York

Lebrun, J., (1970), Physiological requirements and physical modalities of air conditioning by a static concentrated source, *Ph.D thesis, University of Liege*

Lee, C.S., (2003), A theoretical study on VOC source and sink behavior of porous building materials, *Ph.D thesis, Concordia University*

Lin, Y., (1999), POMA - A zonal model for airflow and temperature distribution analysis, *MA.Sc. thesis, Concordia University*

Maref, W., Lacasse, M., Kumaran, M. K., and Swinton, M.C., (2002), Benchmarking of the advanced hygrothermal model – hygIRC with mid scale experiments, *Proceedings of esim2002: 171- 176. Sept. 11-13, Montreal, Canada*

Martin, P.C., and Verschoor, J.D., (1986), cyclical moisture absorption /desorption by building construction and furnishing materials, *Symposium on Air Infiltration, Ventilation and Moisture Transfer, Building Thermal Envelope Coordinating Council, pp.* 59-69, *FortWorth, Texas*

Masel, R.I., (1996), Principles of adsorption and reaction on solid surfaces, *John Wiley &Sons, INC.*

Mendes, N., Ridley, I., Lamberts, R., Philppi, P.C., and Budag, K., (1999), UMIDUS: A PC program for the prediction of heat and moisture transfer in porous building elements. *Building Simulation Conference – IBPSA* 99:277 – 283. Kyoto, Japan

Mendes, N., Lamberts, R., and Philippi, P.C., (2001), Moisture Migration through exterior envelope in Brazil, *Proceedings of Performance of Exterior Envelopes of Whole Buildings VIII.* Clearwater Beach, Florida

Mendonca, KC., Inard, C., Wurtz, E., Winkelmann, F.C., and Allard, F., (2002), A zonal model for predicting simultaneous heat and moisture transfer in buildings, *Proceedings of indoor air 2002. Vol. 4. pp.* 518-523

Molenda, C.H.A., Crausse, P., and lemarchchand, D., (1992), The influence of capillary hystersis effects on the humidity and heat coupled transfer in a non-saturated porous medium, *International Journal of Heat and Mass Transfer Vol. 35 (6), pp.*1385-1396

Musy. M., (1999), Generation automatique de modeles zonaux pour l'Étude du comportment thermo-aeraulique des batiments. *Ph.D thesis: Universite de La Rochelle (FR)*

Musy. M., Wurtz E., Winkelmann F. and Allard F., (2001), Generation of a zonal model to simulate natural convection in a room with a radiative/ convective heater, *Building and Environment* 36, *pp.*589-596

Nielsen, P.V., (1989), Airflow simulation techniques – progress and trends, *Proceedings of the 10th AIVC Conference, Dipoli, Finland, pp.* 203-223

Nofal, M., Straver, M., and Kumaran, K., (2001), Comparison of four hygrothermal models in terms of long-term performance assessment of wood-frame constructions, *Solutions to Moisture Problems in Building Enclosures, Proceedings of the 8th Conference on Building Science and Technology, Toronto, Canada, pp.* 119-138

Ojanen, T. and Kohonen, R., (1989), Hygrothermal influence of air convective in wall structures. *Proceedings of Thermal Performance of the Exterior Envelopes of Buildings IV, pp.* 234-242

Ojanen, T., Salonvaara, M., Kohonen, R., and Nieminen, J., (1989), Moisture transfer in building structures: numerical methods (English Traslation)/ Kosteuden siirtyminen rakenteissa Lakentamentelmat, Technical Research Center of Finland, Report no. 595, (referred in Lee, 2004)

Ojanen, T., Kohonen, R., and Kumaran, M.K., (1994), Modeling heat, air and moisture transport through building materials and components. Chapter 2 in Moisture Control in Buildings, Trechsel, H., ASTM Manual Series MNL 18

Patankar, S.V., (1980), *Numerical heat transfer and fluid flow*, McGraw-Hill Company, *pp.*64-68

Pederson, C.R., (1990), Combined heat and moisture transfer in building materials, *Report No. 214*, Thermal insulation laboratory, Technical University of Denmark, Denmark

Press, W. H., (1992), *Numerical recipes in FORTRAN 90*, Cambridge (England), New York, NY, USA: Cambridge University Press

Quenard, D., and Sallee, H., (1991), Water vapor adsorption and transfer in microporous building materials: a network simulation, *Proceedings of Building Simulation'91 Conference, Nice, France, pp.* 31-36

Rodriguez, E., and Allard, F., (1995), Zonal modeling for nature ventilation, *Final report on Ventilation Thermal Mass Subtask in PASCOOL, Chapter 7*

Rutman, E., Inard, C., Bailly, A. and Allard, F., (2002), Prediction of global comfort in air conditioned building with a zonal model, *Proceedings: 9th International Conference on Indoor air Quality and Climate, Monterey, California, Vol. 3, pp.* 724-729

Ruthven, D.M., (1984), Principles of Adsorption and Adsorption Processes, *John Wiley & Sons, Inc.*

Satterfield, C.N., (1970), Mass Transfer in Heterogeneous Catalysis, *MIT Press*

Sherwood, T.K., and Pigford, R.L., (1952), Absorption and Extraction, *New York: McGraw-hill Co.*

Sowell, E.F., and Haves, P., (2001), Efficient solution strategies for building energy simulation. *Energy and Buildings Vol.33, pp.* 309-317

Spolek, G.A., and Piroozmandi, F., (1989), Measurement of unsaturated wood permeability by transient flow methods, Water Vapor Transmission Through Building Materials and Systems: Mechanisms and Measurements, ASTM STP 1039, Trechesel, H.; Bomberg, M., Eds., *American Society for Testing and Materials, pp.* 114-121

Spooner, D.C., (1983), The practical relevance of mechanism of water vapor transport in porous building materials, *Proceedings: Autoclaved aerated concrete, moisture and properties, Amsterdam, Netherlands, pp.* 27-41

Straube, J. and Burnett, E., (2001), Overview of Hygrothermal (HAM) analysis methods, *Chapter 5, ASTM Manual 40- Moisture Analysis and Condensation Control in Building Envelopes, American Society of Testing and Materials, Philadelphia*

Swami, M.V., Chandra, S., (1988), Correction for pressure distribution on building and calculations of natural-ventilation airflow, *ASHRAE Transactions. Vol. 94(1), pp.*243-266

Teodosiu, C., Hohota, R., Rusaouen, G., and Woloszyn, M., (2003), Numerical prediction of indoor air humidity and its effect on indoor environment, *Building and Environment* 38, *pp.*655-664

Thomas, W.C. and Burch, D.M., (1990), Experimental validation of a mathematical model for predicting water vapor sorption at interior building surfaces, *ASHRAE Transactions. Vol. 96(1), pp.*487-496

Tsuchiya, T., (1980), Infiltration and indoor air temperature and moisture variation in a detached residence. *Journal of the Society of Heating, Air-Conditioning and Sanitary Engineers of Japan 54 No.11, pp.*13-19

Wong, S.P.W., and Wang, S.K., (1990), Fundamentals of simultaneous heat and moisture transfer between building envelope and the conditioned space air. *ASHRAE Transactions. Vol. 96(2), pp.*73-83

Wurtz, E., Musy, M., and Mora, L., (1999a), Introduction of specific law in zonal model to describe temperature fields and sir flow patterns in ventilated buildings. *Journal of Human-Environment System, Vol. 3(1), pp.*43-59

Wurtz, E., Nataf, J-M., and Winkelmann, F., (1999b), Two and three dimensional natural and mixed convection simulation using zonal models in buildings. *International Journal of Heat and Mass Transfer, Vol. 40, pp.*923-940

Young, D.M. and Crowell, A.D., (1962), Physical Adsoption of Gases, Butterworth & Co. Ltd.

APPENDIX I

Gauss-Seidel Method

The Gauss-Seidel method is a technique for solving the n equations of the linear system of equations, one at a time in sequence, and uses previously computed results as soon as they are available,

$$x_i^{(k)} = \frac{b_i - \sum_{j<i} a_{ij} x_j^{(k)} - \sum_{j>i} a_{ij} x_j^{(k-1)}}{a_{ii}} \qquad \text{(i)}$$

There are two important characteristics of the Gauss-Seidel method should be noted. Firstly, the computations appear to be serial. Since each component of the new iterate depends upon all previously computed components, the updates cannot be done simultaneously as in the Jacobi method. Secondly, the new iterate $x^{(k)}$ depends upon the order in which the equations are examined. If this ordering is changed, the components of the new iterates (and not just their order) will also change.

In terms of matrices, the definition of the Gauss-Seidel method can be expressed as

$$x^{(k)} = (D - L)^{-1}(ux^{(k-1)} + b) \qquad \text{(ii)}$$

where the matrices D, L, and U represent the diagonal, strictly lower triangular, and strictly upper triangular parts of A, respectively.

The Gauss-Seidel method is applicable to strictly diagonally dominant, or symmetric positive definite matrices A.

Pseudocode:
Choose an initial guess $x^{(0)}$ to the solution x.
for $k = 1, 2, \ldots$
  for $i = 1, 2, \ldots, n$
    $\sigma = 0$
    for $j = 1, 2, \ldots, i-1$
      $\sigma = \sigma + a_{ij} x_j^{(k)}$
    end
    for $j = i+1, \ldots, n$
      $\sigma = \sigma + a_{ij} x_j^{(k-1)}$
    end
    $x_i^{(k)} = (b_i - \sigma)/a_{ii}$
  end
  check convergence; continue if necessary.
end